QCD@LHC2015

Queen Mary,
University of London

September 1-5, 2015

Results on Minimum Bias Interactions, Underlying Events and Particles Production from ATLAS

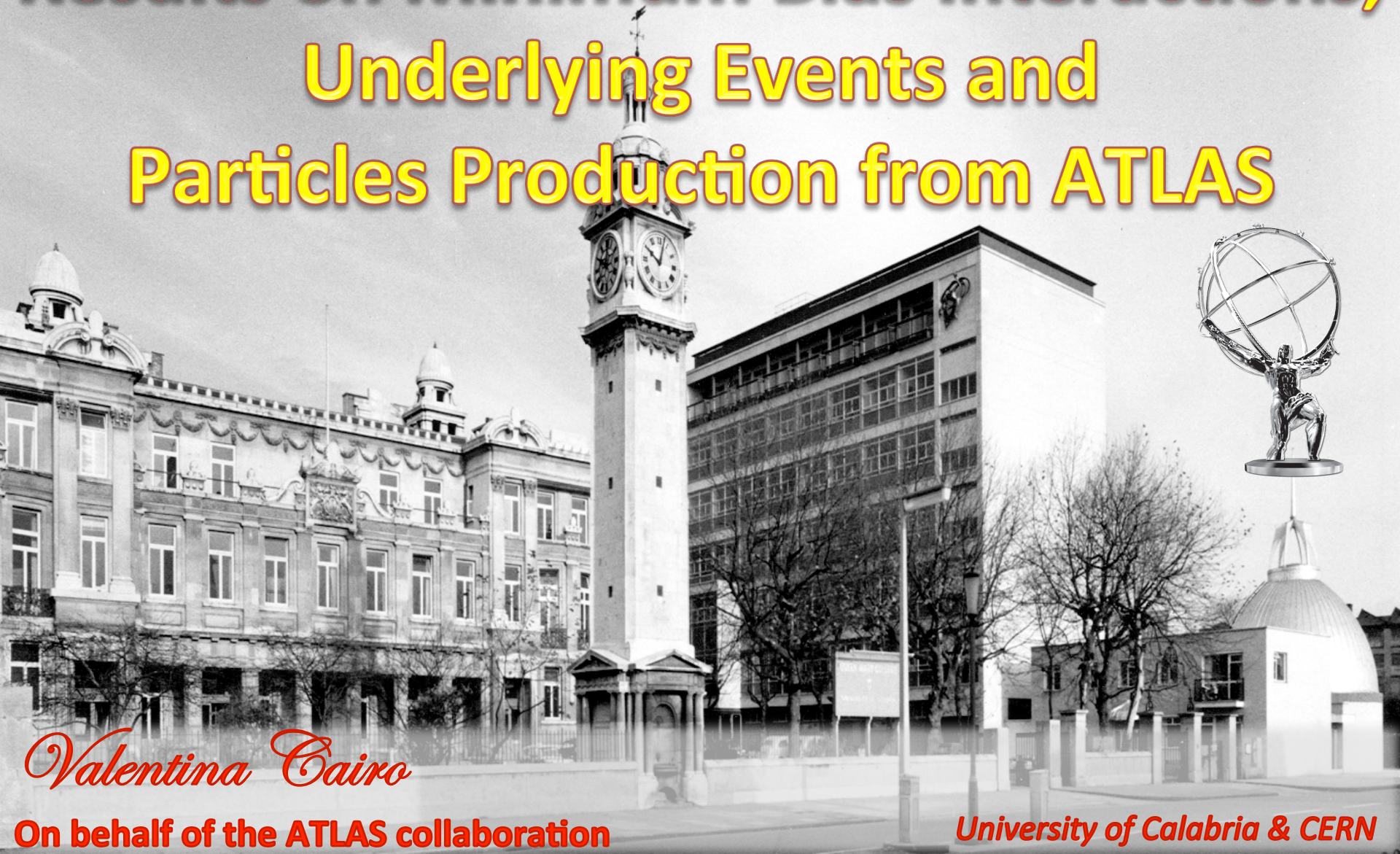

Valentina Cairo

On behalf of the ATLAS collaboration

University of Calabria & CERN

Outline

- The ATLAS detector is a multi-purpose detector with a tracking system ideal for the measurement of particles kinematics
  - New **Insertable B-Layer** (**IBL**) added to the tracking system during Long Shutdown 1

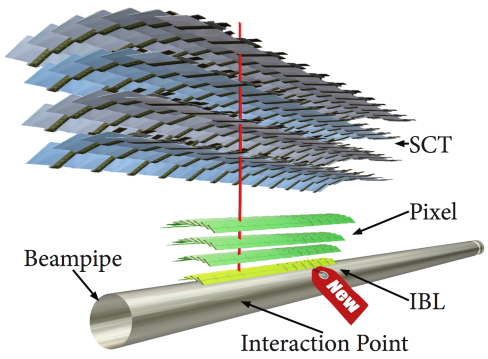

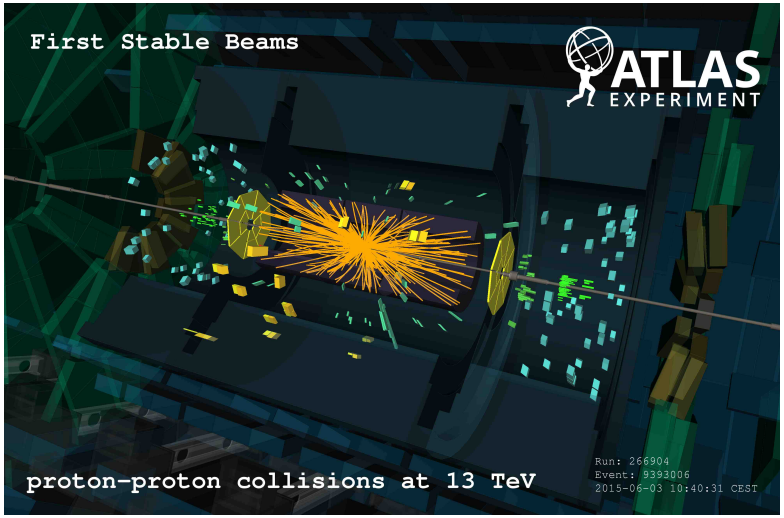

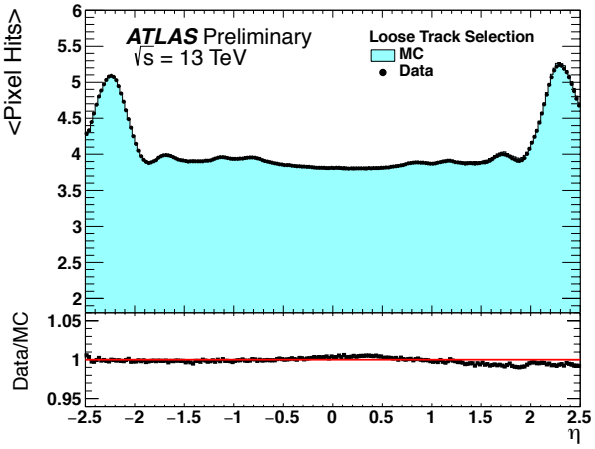

- In this talk
  - Focus on 13 TeV results and comparison for:
    - **Minimum Bias Analysis**
    - **Underlying events**
  - Focus on 0.9 and 7 TeV results and comparison for:
    - **Bose-Einstein Correlation**

- <u>Not covered here but in another specific talk:</u>
  - Two-particle correlation and ridge effect

Minimum Bias Analysis

- Inclusive charged-particle measurements in pp collisions provide insight into the strong interaction in the low energy, non-perturbative QCD region

- Inelastic pp collisions have different compositions

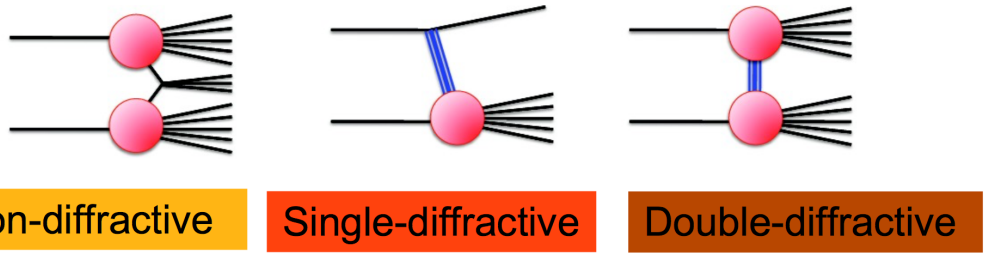

- Main source of background when more than one interaction per bunch crossing

- Perturbative QCD can not be used for peripheral interactions
  - ND described by QCD-inspired phenomenological models (tunable)
  - SD and DD hardly described and little data available

Goal:

Measure spectra of unfolded primary charged particles

Inclusive measurement – do not apply strong model dependent corrections

Analysis Overview

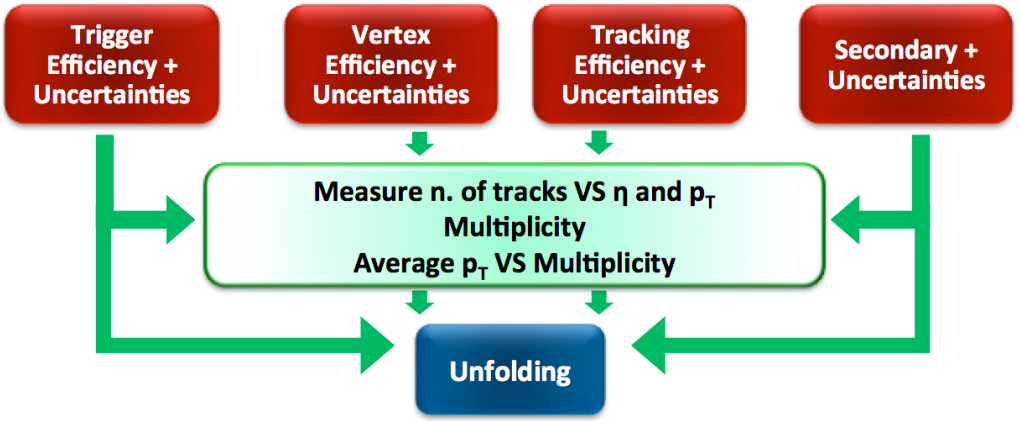

Published results at 0.9, 2.76, 7 TeV (http://arxiv.org/abs/1012.5104)

Tracks VS η

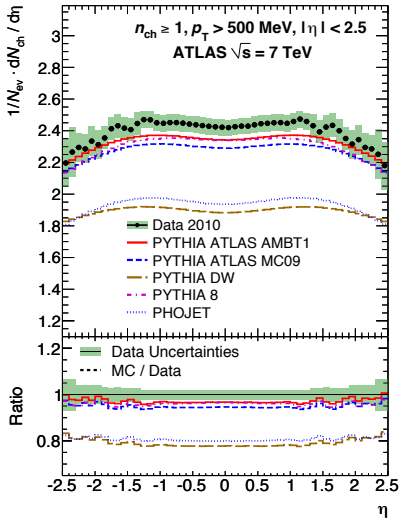

Tracks VS p_T

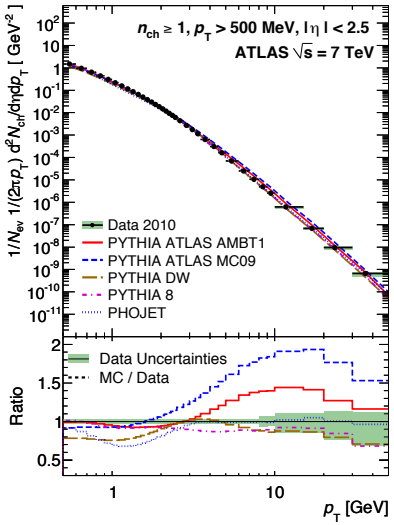

Multiplicity

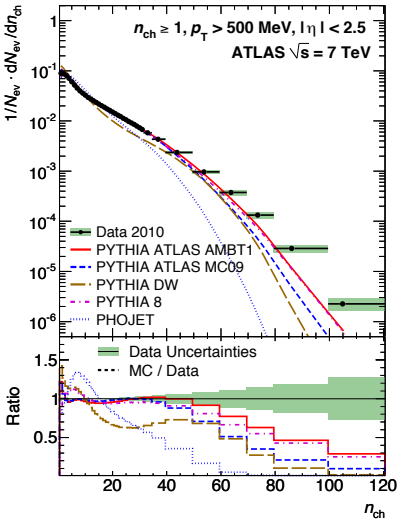

<p_T>VS Multiplicity

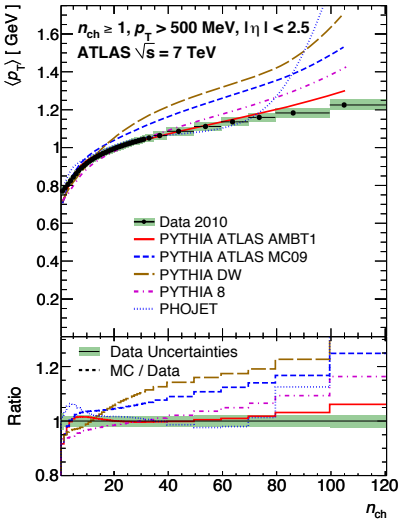

- Previous tunes under-estimated the rate of charged particles, their multiplicity and mismodelled their p_T spectrum
- New analysis performed with 13 TeV data (June 2015) - ATLAS-CONF-2015-028

Minimum Bias Analysis at 13 TeV: Event Selection

- Accepted on single-arm Minimum Bias Trigger Scintillator (MBTS)
- Primary vertex (2 tracks with p_T >100 MeV)
- Veto on any additional vertices with ≥ 4 tracks
- At least one selected track:
  - p_T > 500 MeV and $|\eta|$ < 2.5 (note track reconstruction runs with 100 MeV)
  - At least 1 Pixel hit
  - At least 6 SCT hits
  - IBL hit required
  - $|d_0^{BL}|$ < 1.5 mm (transverse impact parameter w.r.t beam line)
  - $|\Delta z_0 \sin\vartheta|$ < 1.5 mm (Δz_0 is the difference between track z_0 and vertex z position)
  - Track fit χ^2 probability > 0.01 for tracks with p_T > 10 GeV

Using the two 13 TeV low mu (<μ> ~ 0.005) runs:

168 μb^{-1}
8,870,790 events selected, with
106,353,390 selected **tracks**!

Track Reconstruction Efficiency

$$\epsilon_{\mathrm{trk}}(p_{\mathrm{T}},\eta) = \frac{N_{\mathrm{rec}}^{\mathrm{matched}}(p_{\mathrm{T}},\eta)}{N_{\mathrm{gen}}(p_{\mathrm{T}},\eta)}$$

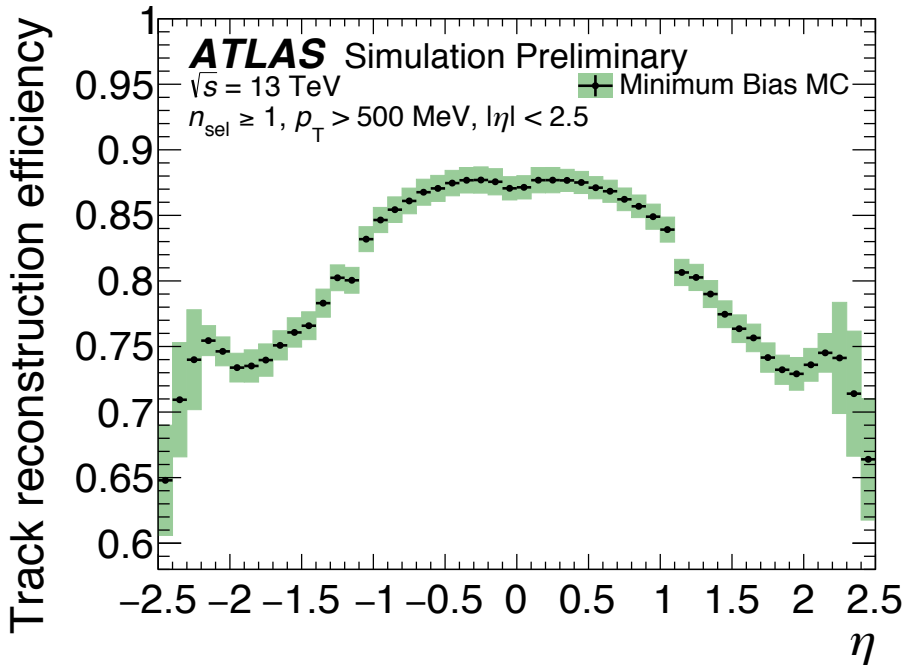

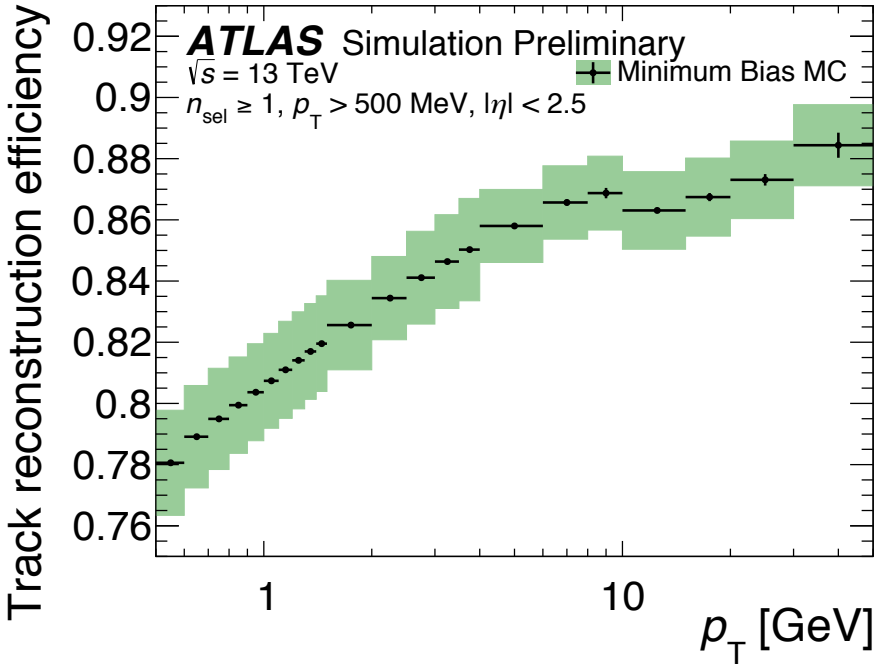

- Systematic uncertainty dominated by the knowledge of the material distribution
- Multiple methods used to constrain the uncertainty
  - Hadronic Interaction Rate
  - Photon Conversion Rate
  - SCT Extension Efficiency
- Systematics on tracking efficiency evaluated from simulated samples -> 1.1% at η=0

Non-Primary Tracks Estimation

- Non primary tracks are the biggest background
  - Rate measured in data by performing a fit to the transverse impact parameter distribution
  - 2.2% ± 0.6% of reconstructed tracks within the signal region
- High p_T tracks
  - Measurable fraction of the tracks originate from low p_T tracks (scattering, in flight decays)
  - Ability to select and remove these tracks assessed in data
  - At most 1% of tracks between 30-50 GeV

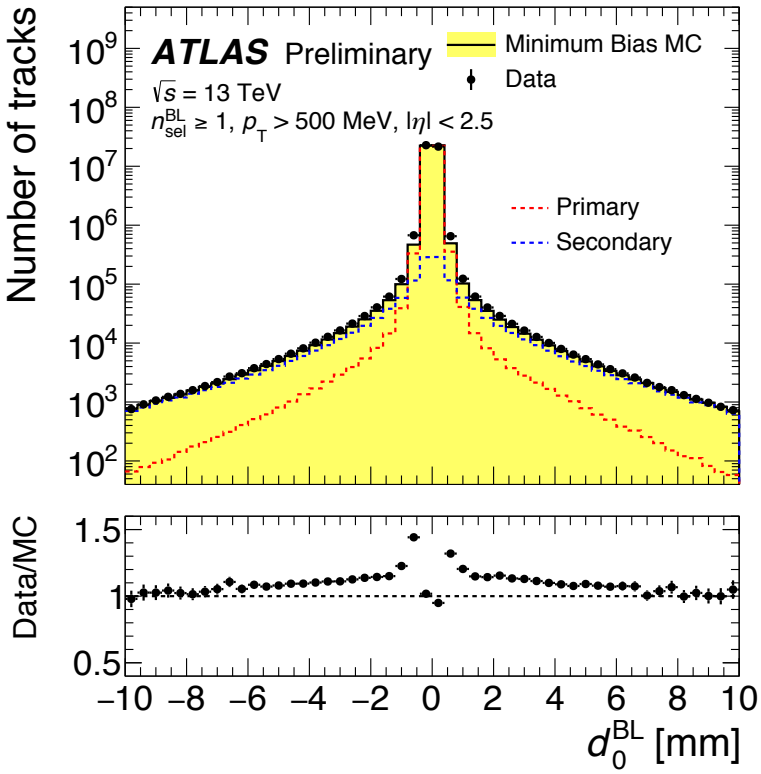

new

Strange Baryons

- Particles with lifetime 30 ps < τ < 300 ps (strange baryons) are no longer considered primary particles in the analysis, decay products are treated like secondary particles

- Low reconstruction efficiency (<0.1%) and large variations in predicted rates lead to a model dependence

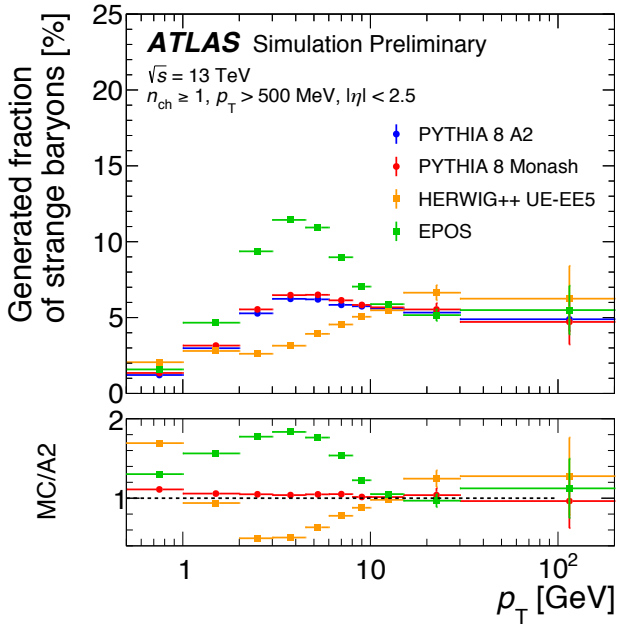

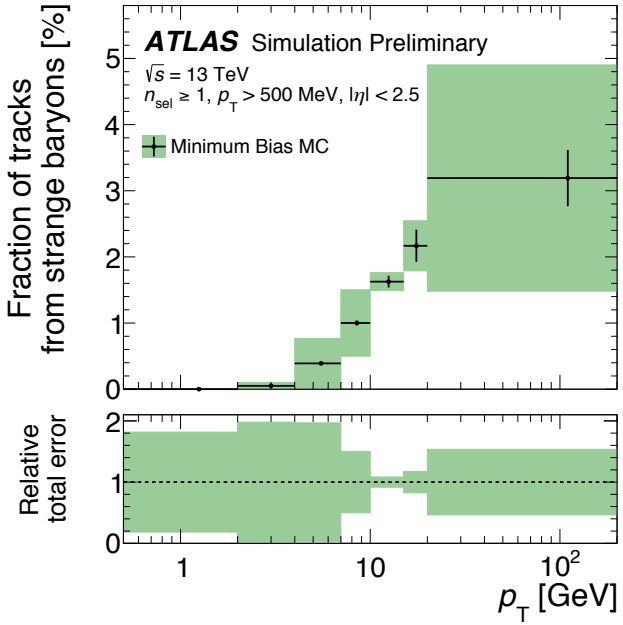

Corrections

- Trigger and Vertex efficiency: event-wise correction

$$w_{\mathrm{ev}}(n_{\mathrm{sel}}^{\mathrm{BL}}, \eta) = \frac{1}{\varepsilon_{\mathrm{trig}}(n_{\mathrm{sel}}^{\mathrm{BL}})} \cdot \frac{1}{\varepsilon_{\mathrm{vtx}}(n_{\mathrm{sel}}^{\mathrm{BL}}, \eta)},$$

- Tracking efficiency: track-wise correction

$$w_{\mathrm{trk}}(p_{\mathrm{T}}, \eta) = \frac{1}{\varepsilon_{\mathrm{trk}}(p_{\mathrm{T}}, \eta)} \cdot (1 - f_{\mathrm{sec}}(p_{\mathrm{T}}, \eta) - f_{\mathrm{sb}}(p_{\mathrm{T}}) - f_{\mathrm{okr}}(p_{\mathrm{T}}, \eta)),$$

f_{sec}: secondary tracks

f_{sb}: strange baryons

f_{okr}: outside kinematic range

- Bayesian unfolding to correct both n_{ch} and p_T

- Mean p_T vs n_{ch} bin-by-bin correction of average p_T, then n_{ch} migration

Final MinBias Results

$dN_{ch}/d\eta$

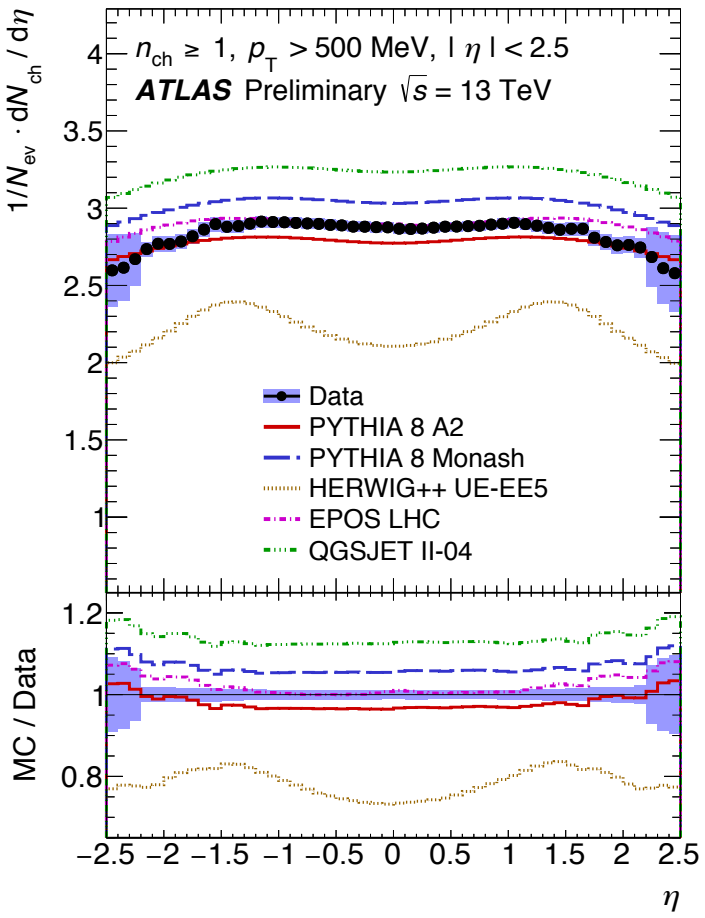

- Models differ mainly in normalisation, shape similar, exception is HERWIG tuned entirely on UE
- Measurement spans 10 orders of magnitude
- Some Models/ Tunes give remarkably good predictions (EPOS, Pythia)

$d^2N_{ev}/d\eta dp_T$

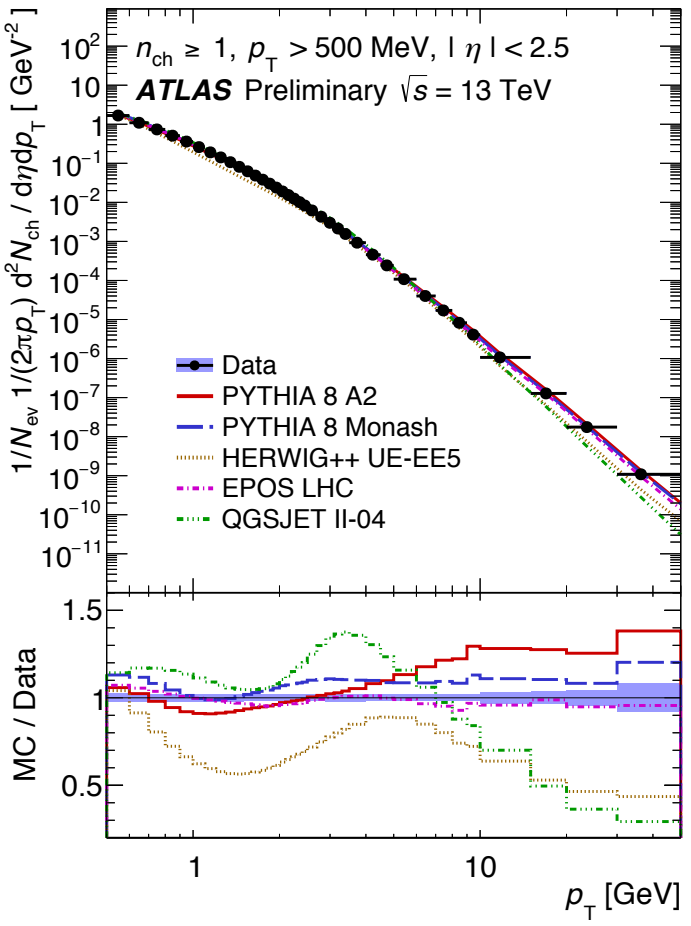

Final MinBias Results

dN_{ev}/dn_{ch}

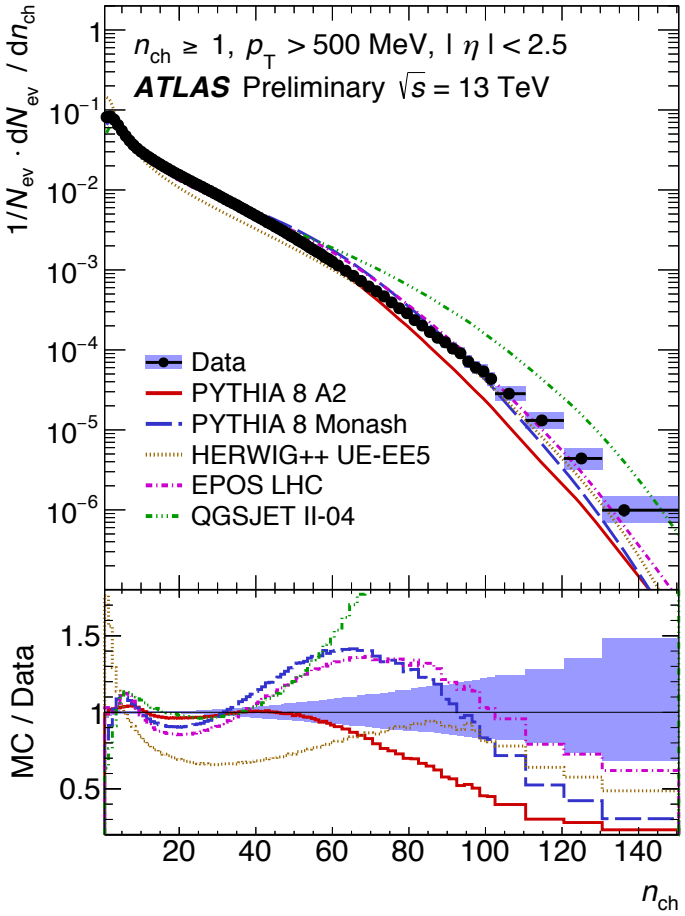

- Low n_{ch} not well modelled by any MC; large contribution from diffraction
- Models without colour reconnection (QGSJET) fail to model scaling with n_{ch} very well

$\langle p_T \rangle$ VS n_{ch}

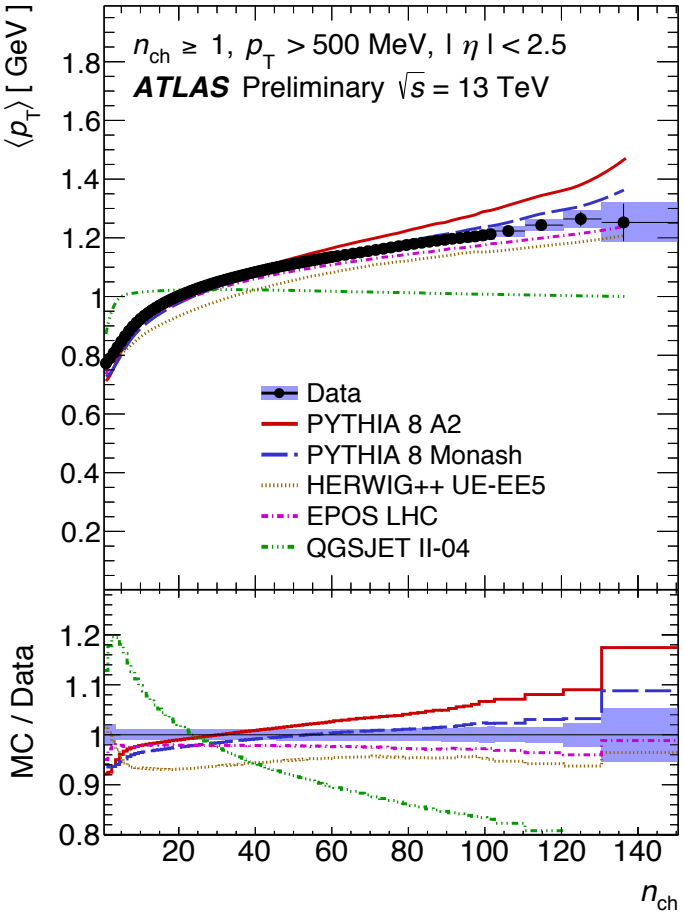

Final MinBias Results

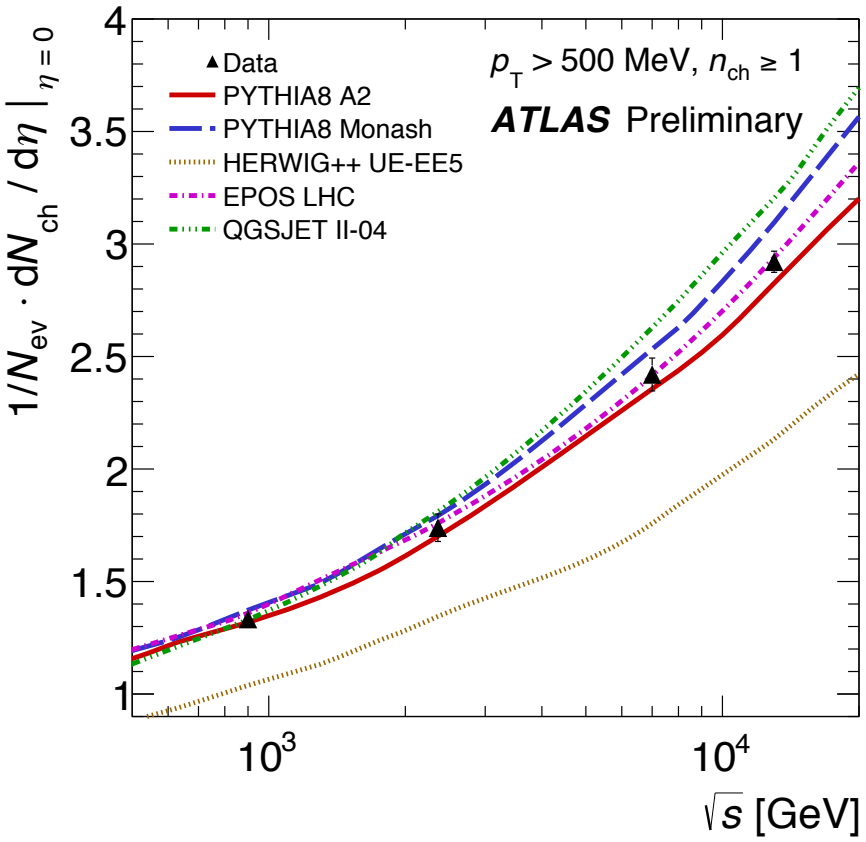

The mean number of charged particles increases by a factor of 2.2 from 0.9 TeV to 13 TeV!

- Analysis of additional phase spaces is ongoing:
  - Reduced: $|\eta| < 0.8$ for comparison to the various detectors
  - Extended: $p_T > 100$ MeV to really test diffractive regime

Underlying Events

- The underlying event (UE) is defined as the activity accompanying any hard scattering in a collision event:
  - Partons not participating in a hard-scattering process (beam remnants)
  - multiple parton interactions (MPI)
  - Initial and final state gluon radiation (ISR, FSR)

- These soft interactions cannot be calculated with perturbative QCD:
  - Free parameters to be tuned using data

- Leading object can be defined variously:
  - Leading jet , Z (p_T), Leading track in Minimum Bias like events

- Preliminary 13 TeV analysis based on leading track:
  - same dataset and same event and track selection as the MinBias analysis with an additional requirement: leading track with a p_T of at least 1 GeV
  - Results presented at detector level, without any correction (the width of the vertex distribution along the *z* axis in MC is reweighted to match the data)
  - The tracking efficiency uncertainty is about 2% or less
  - No correction for secondary tracks is performed

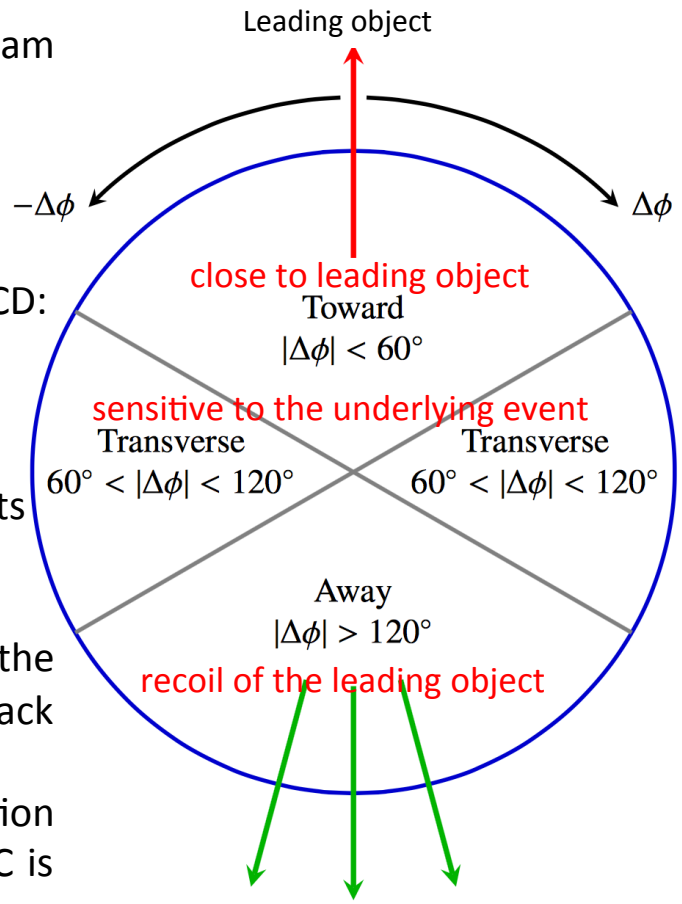

Underlying Events at 7 TeV: Jets and Z

Σp_T for underlying events vs leading jet and Z p_T:

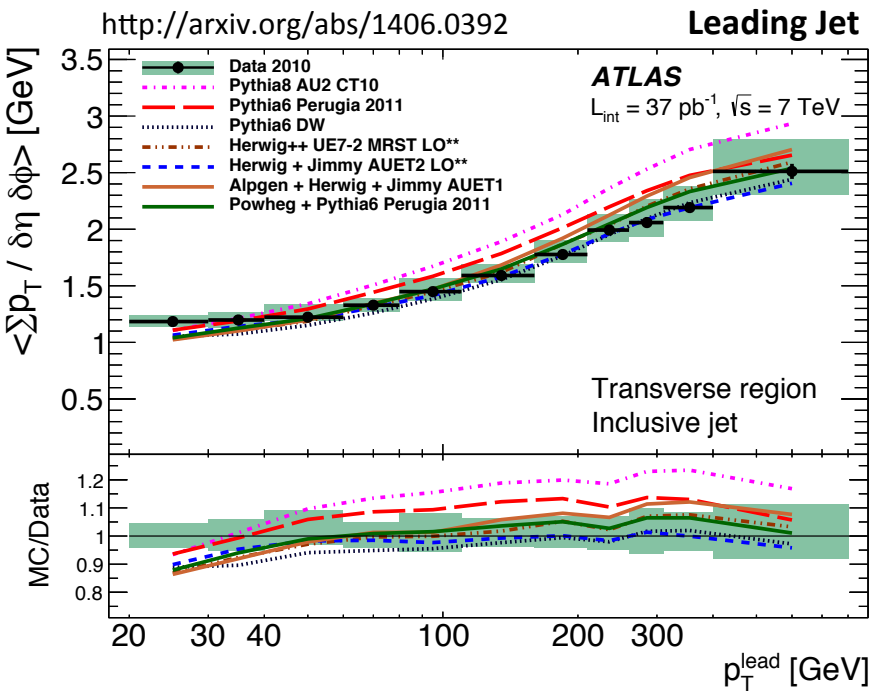

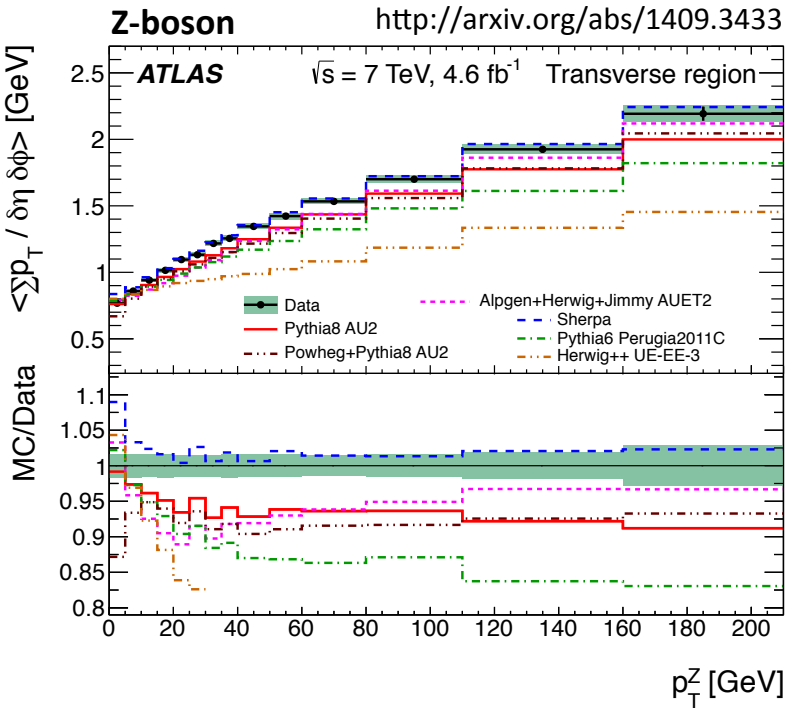

The tracks corresponding to the leptons forming the Z-boson candidate are excluded.

- Not perfect agreement between data and simulation, Herwig better than Pythia (old tunes)
- For Z-boson, good description given by Sherpa, followed by PYTHIA 8, ALPGEN and POWHEG
- Multi-leg and NLO generator predictions are closer to the data than most of the pure parton shower generators -> these regions are affected by the additional jets coming from the hard interaction

Underlying Events at 7 TeV: Jets, Z and Tracks

Track density and Σp_T for underlying events vs leading jet or leading track or Z p_T:

http://arxiv.org/abs/1409.3433

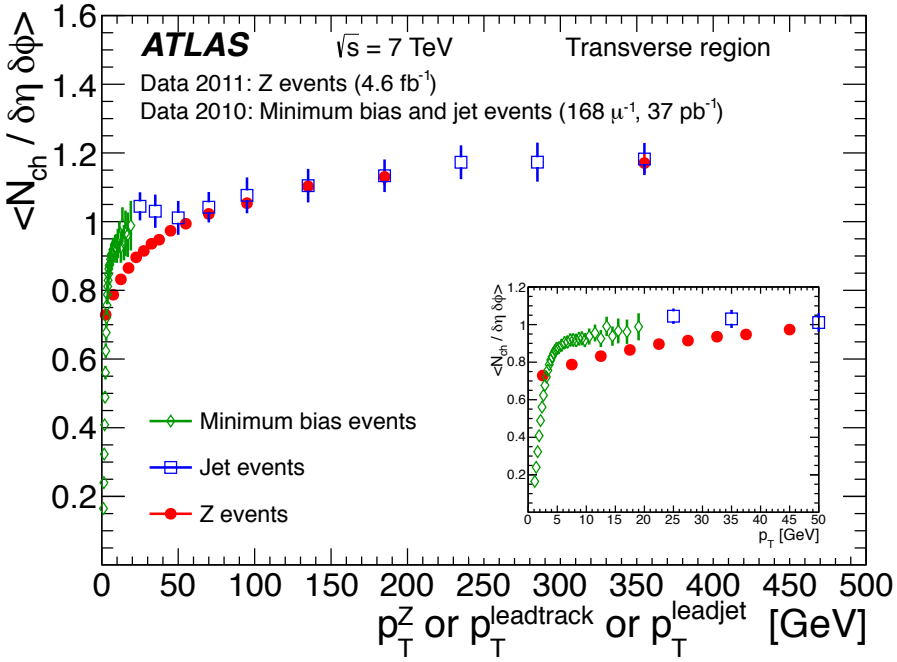

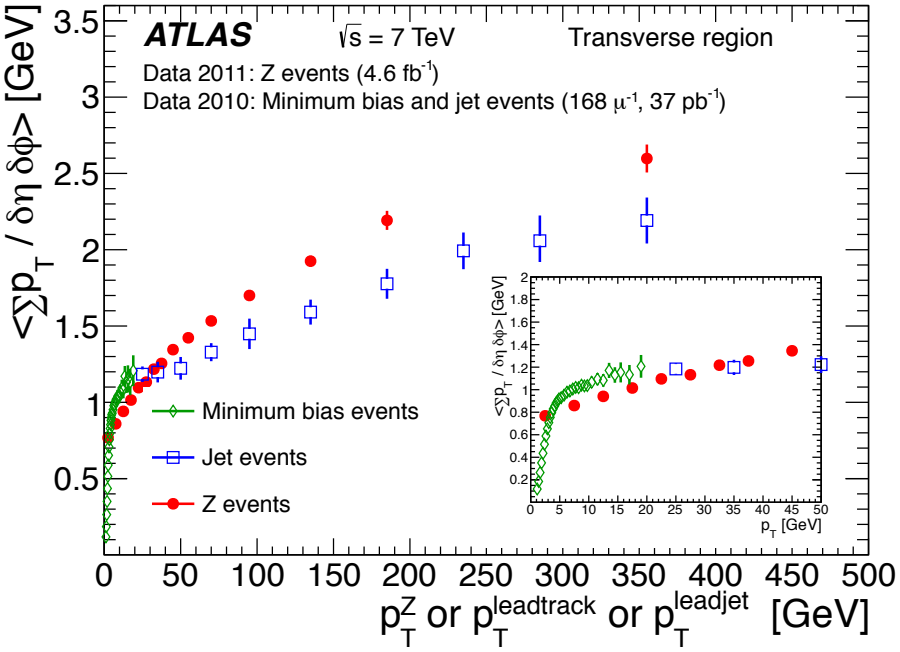

- Data are compatible between the different definitions
- Transition between leading track and jet
- In the track density distribution, Z-bosons and jets agree well at high p_T

Underlying Events at 13 TeV: Σp_T and N_{ch} VS $|\Delta\phi|$ (track)

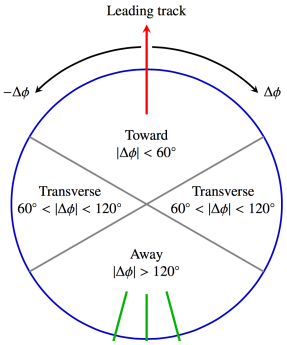

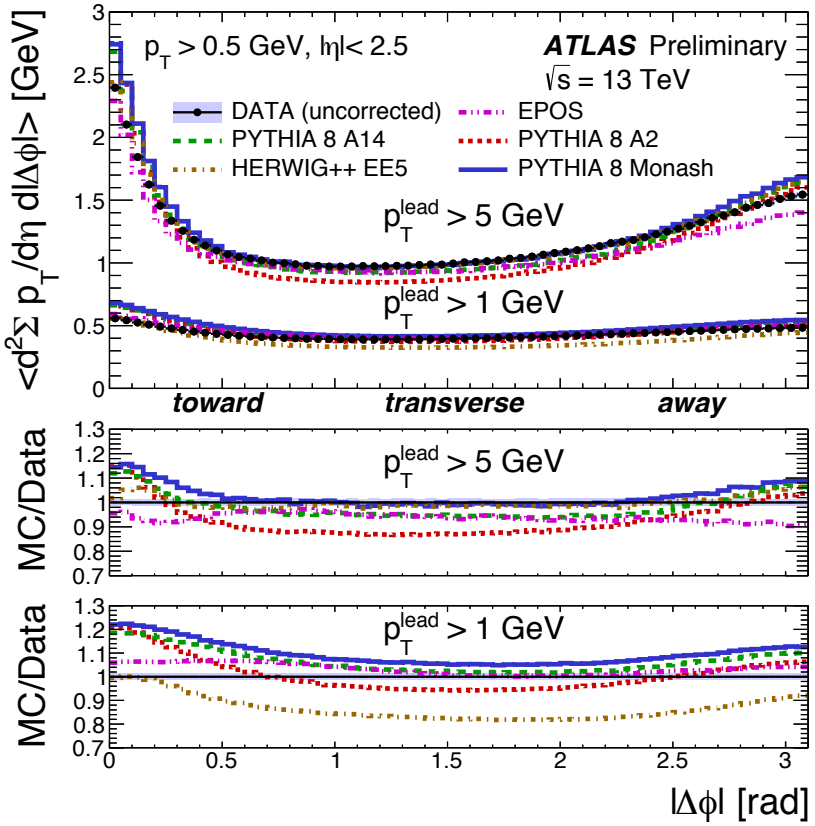

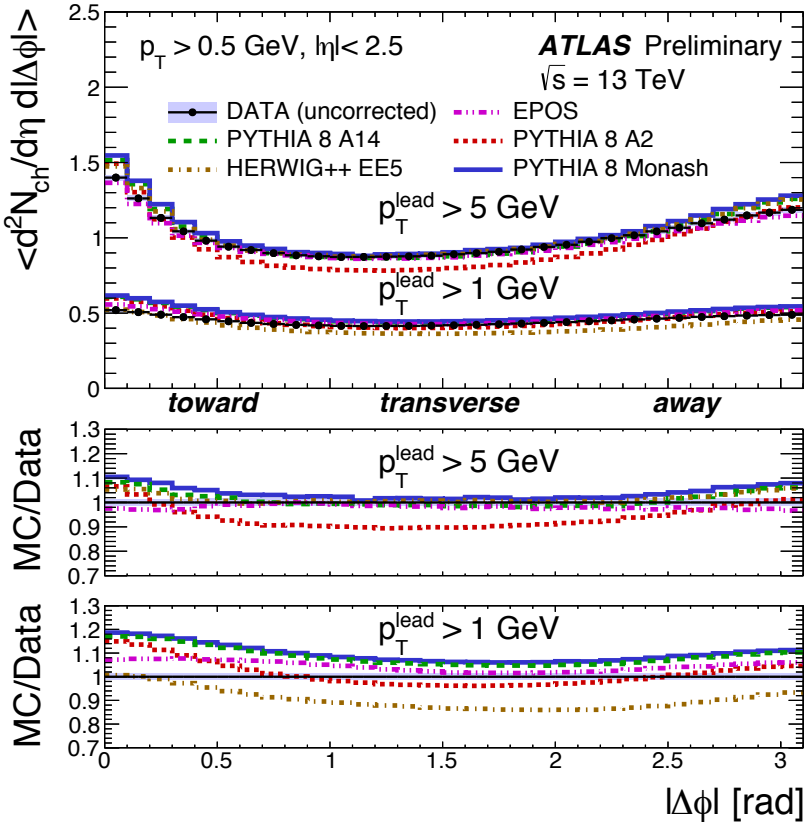

- Good Data/MC agreement with MinBias Tune (A2) at p_T-lead > 1 GeV
- Good Data/MC agreement with Underlying Event Tunes (Herwig++, Monash, A14) at p_T-lead > 5 GeV

Underlying Events at 13 TeV
Σp_T and N_{ch} VS p_T (track)

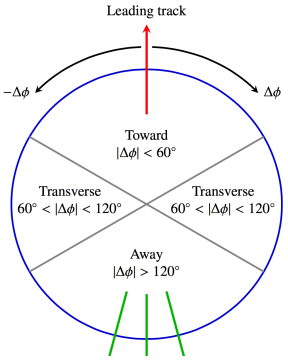

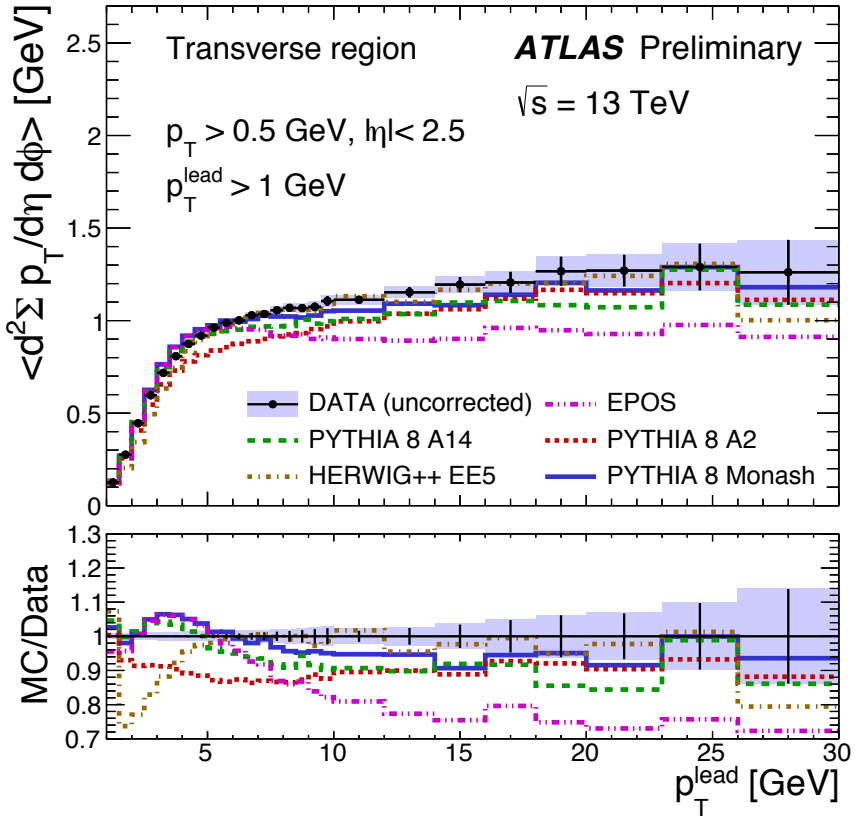

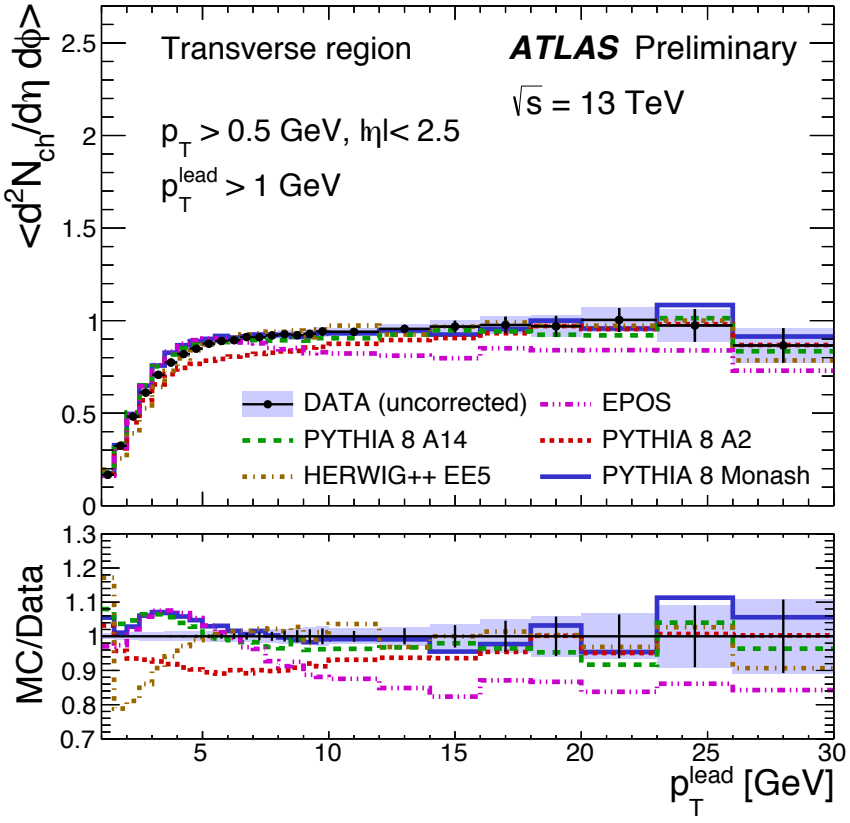

- None of the models describes the initial rise well
- From 10 GeV quite good description for the UE Tunes
- EPOS 15% off in the plateau

arXiv:1502.07947

Bose-Einstein Correlation

- Particle correlations play an important role in the understanding of multiparticle production
- Correlations between identical bosons, called **Bose-Einstein Correlations** (**BEC**), are a well-known phenomenon in high-energy and nuclear physics

$$C_2(p_1, p_2) = \frac{\rho(p_1, p_2)}{\rho_0(p_1, p_2)}$$

Two-particle density function

Reference density function constructed to exclude BEC effects

Four-momenta of two identical bosons

- They represent a sensitive probe of the space-time geometry of the hadronization region and allow the determination of the size and the shape of the source from which particles are emitted
- Studies of one-dimensional BEC effects in pp collisions in the kinematic range $p_T > 500$ MeV and $|\eta| < 2.5$ at centre-of-mass energies of 0.9 and 7 TeV are presented
- The studies are extended to the region of high-multiplicities available thanks to the high-multiplicity track trigger

$$Q^2 = -(p_1 - p_2)^2 \rightarrow C_2(Q) = \frac{\rho(Q)}{\rho_0(Q)} = C_0[1 + \Omega(\lambda, QR)](1 + \varepsilon Q) \rightarrow R_2(Q) = \frac{C_2(Q)}{C_2^{MC}(Q)} = \frac{\rho(++,--)}{\rho(+-)} \Big/ \frac{\rho^{MC}(++,--)}{\rho^{MC}(+-)}$$

The BEC effect is usually described by a function with two parameters:

- effective radius **R**
- strength parameter **λ**

In this studies, the density function is calculated for like-sign charged-particle pairs, with both the ++ and -- combinations included

arXiv:1502.07947

Bose-Einstein Correlation

- Two parameterizations of the Ω(λ,QR) function have been investigated:

$$\Omega = \lambda \cdot \exp\left(-R^2Q^2\right)$$ → Goldhaber, spherical shape with a Gaussian distribution of the source

$$\Omega = \lambda \cdot \exp\left(-RQ\right)$$ ⇢ Exponential, radial Lorentzian distribution of the source

overestimate of $\rho \to \pi^+\pi^-$ decays in the Monte Carlo simulation

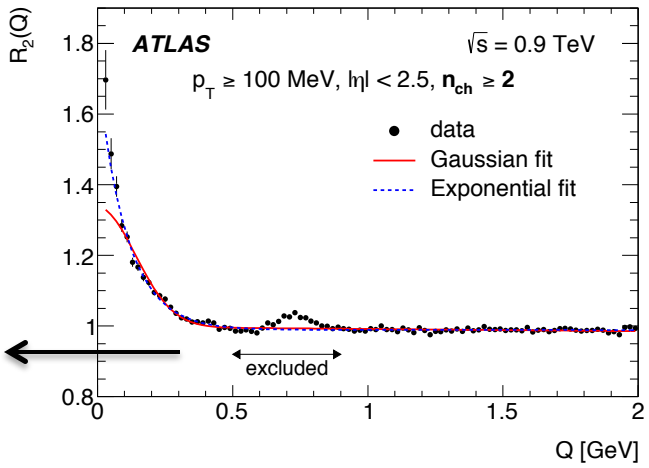

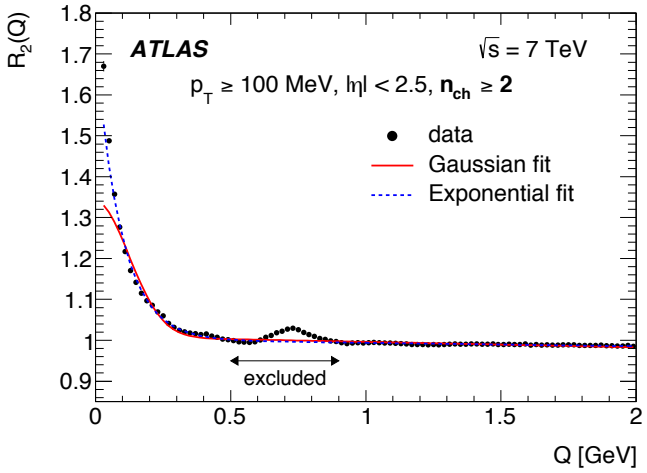

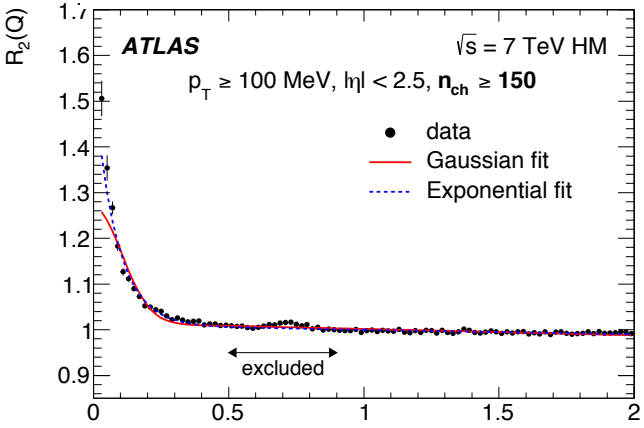

$$\lambda = 0.74 \pm 0.11,\ R = 1.83 \pm 0.25 \text{ at } \sqrt{s} = 0.9 \text{ TeV for } n_{\text{ch}} \geq 2,$$
$$\lambda = 0.71 \pm 0.07,\ R = 2.06 \pm 0.22 \text{ at } \sqrt{s} = 7 \text{ TeV for } n_{\text{ch}} \geq 2,$$
$$\lambda = 0.52 \pm 0.06,\ R = 2.36 \pm 0.30 \text{ at } \sqrt{s} = 7 \text{ TeV for } n_{\text{ch}} \geq 150.$$

Consistent with CMS and ALICE results

arXiv:1502.07947

Bose-Einstein Correlation

- Multiplicity dependence (only the exponential fit is shown)

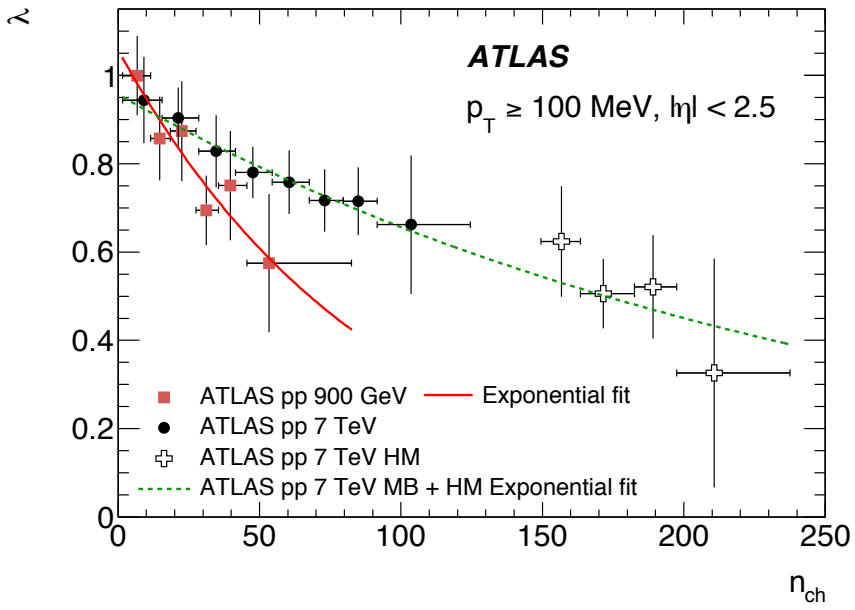

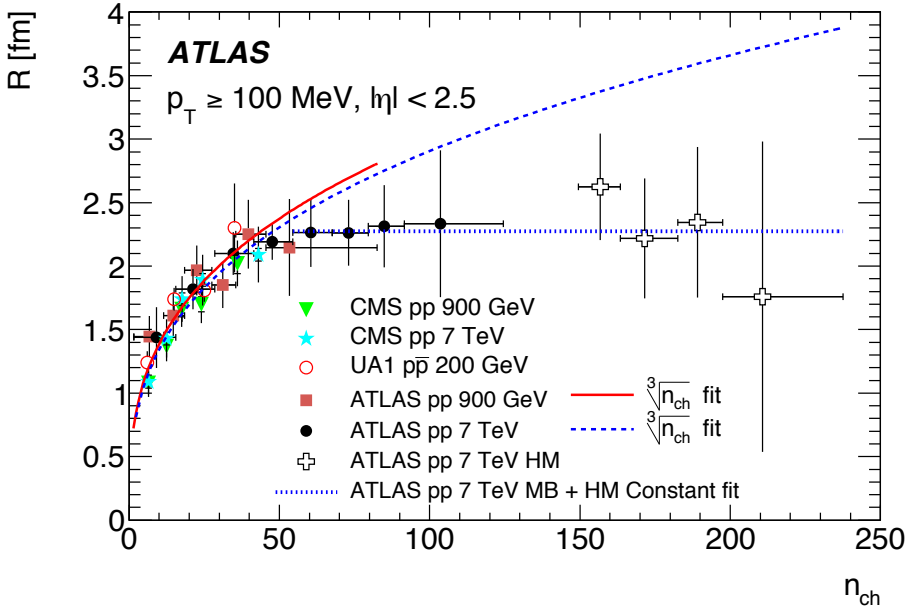

- The λ parameter decreases with multiplicity, faster for 0.9 TeV than for 7 TeV interactions
- λ = 0 -> fully correlated
- λ = 1-> chaotic

- The R parameter increases with multiplicity up to about nch ≃ 50 independently of the center of mass energy
- For higher multiplicities, the measured R parameter is observed to be independent of multiplicity -> saturation at n_{ch}~ 70 observed for the first time!

Summary

ATLAS: good benchmark to study soft QCD!

- **Minimum Bias Studies:**
  - Charged Particle Multiplicities @ 13 TeV
    - $p_T > 500$ MeV, $|\eta| < 2.5$ available results (ATLAS-CONF-2015-028)
      The models have given solid predictions for the latest centre of mass energy
    - $p_T > 100$ MeV, $|\eta| < 2.5$ ongoing studies
    - $p_T > 500$ MeV, $|\eta| < 0.8$ ongoing studies

- **Underlying Event Studies:**
  - Needed for tuning of the soft part of Monte Carlo simulation
  - Latest studies done at 7 TeV: leading jet (Eur.Phys.J. C74 (2014) 2965) and Z (Eur.Phys.J. C74 (2014) 2965)
  - New comparisons for Underlying Event with 13 TeV (ATL-PHYS-PUB-2015-019)
    - reasonable agreement of tunes used in ATLAS Monte Carlo with new data

- **Particle Production Studies:**
  - Bose-Einstein Correlations of same sign particles (arXiv:1502.07947, submitted to EPJC)
    - saturation effect in the effective radius observed for large n_{ch}

Extra Slides

Trigger and Vertex Reconstruction Efficiency

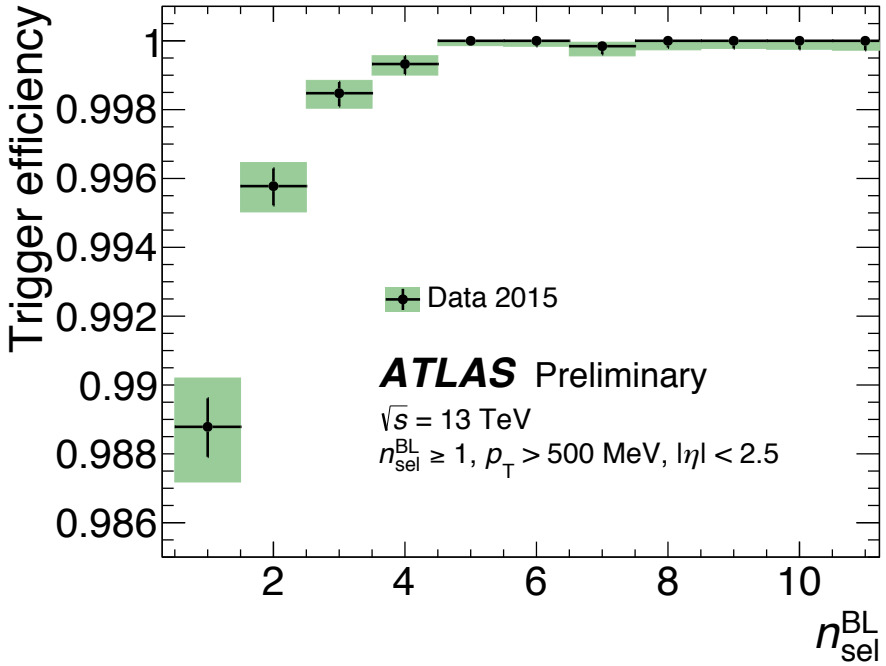

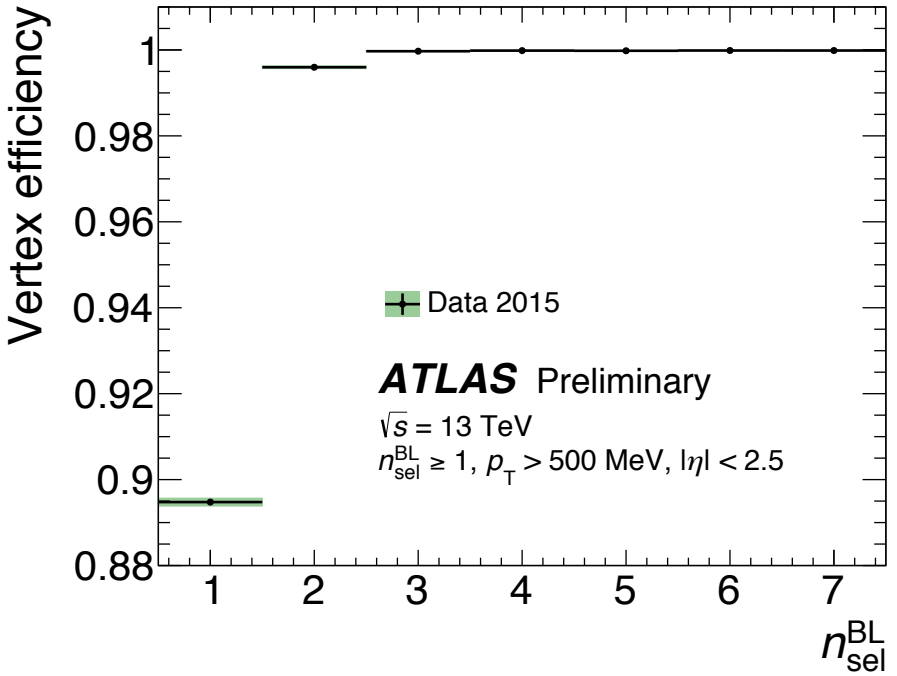

- Evaluated from Data

- Dependence on kinematic quantities has been studied:
  - negligible p_T-dependence
  - visible n_{sel}-dependence
  - **negligible systematic uncertainties**

arXiv:1502.07947

Λ polarisation in the transverse plane

- The Λ hyperons are spin-1/2 particles and their polarization is characterized by a polarization vector **P**. Its component, P, transverse to the Λ momentum is of interest since for hyperons produced via the strong interaction parity conservation requires that the parallel component is zero
- Huge Λ sample allows to measure Λ polarisation P by measuring the decay angle cosθ* between the decay proton and Λ flight directions
- $P(\Lambda) = (1 + \alpha P \cos\theta^*)$; Decay asymmetry : $\alpha = 0.642 \pm 0.013$
- Results:
  - $P(\Lambda) = -0.010 \pm 0.005(\text{stat}) \pm 0.004(\text{syst})$
  - $P(\overline{\Lambda}) = 0.002 \pm 0.006\ (\text{stat}) \pm 0.004(\text{syst})$
- Consistent to previous measurement which expect a degradation of the Λ polarisation at high energy

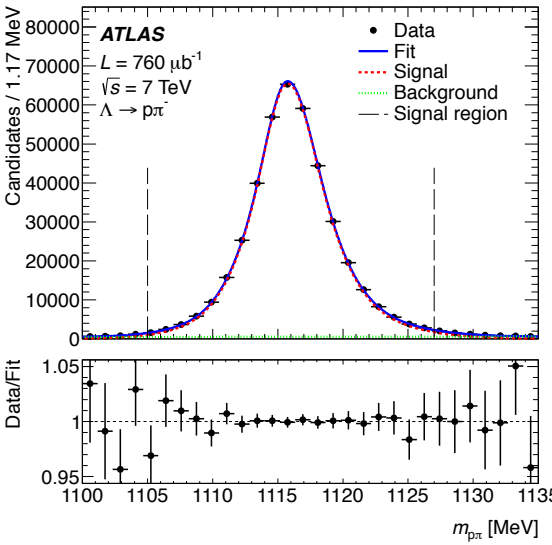

Λ transverse polarization

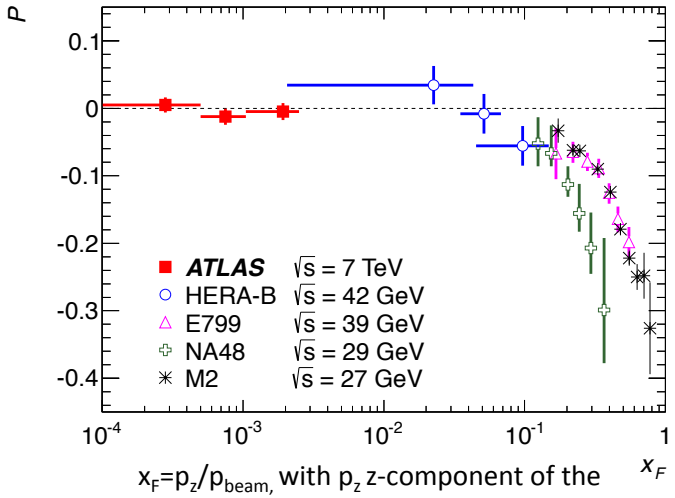

$x_F = p_z/p_{beam}$, with p_z z-component of the Λ momentum and p_{beam} = 3.5 TeV

Trigger Reconstruction Efficiency

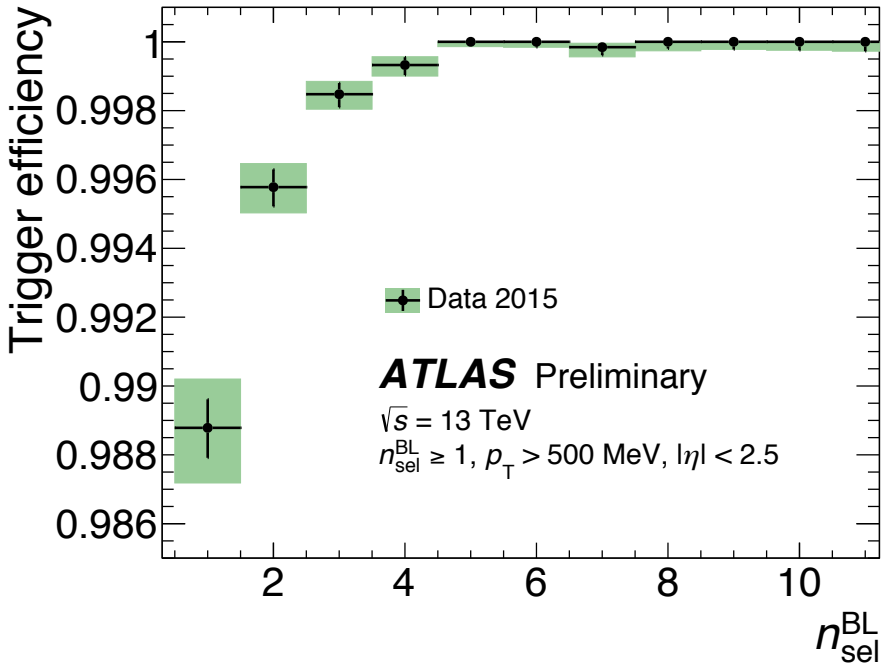

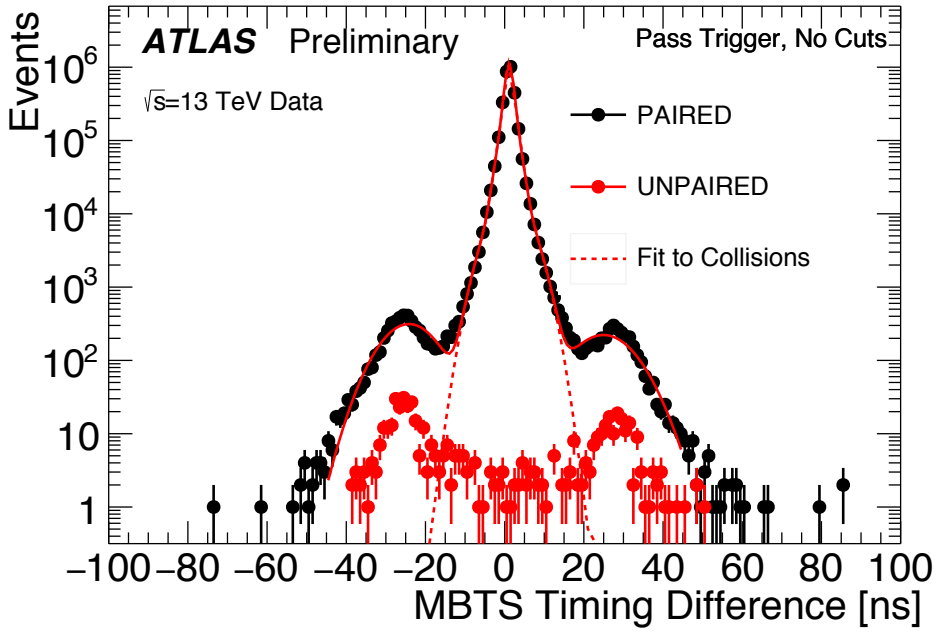

- The difference in the time of the MBTS hits on each side of the detector. Events triggered on UNPAIRED beams (only one of the two beams present at the detector collision point) are shown in red. Events triggered in PAIRED beams (both beams present at the detector collision point) are shown in black. The large central peak in the PAIRED distribution comes from collisions, and the smaller peaks away from 0 ns are caused by non-collision beam background. The MBTS time difference was fit with the sum of five Gaussians. The central peak (sum of 3 Gaussians shown with a dotted red line) is subtracted off, and the remaining contributions are used to normalise the number of observed events from non-collision beam background.

Vertex Reconstruction Efficiency

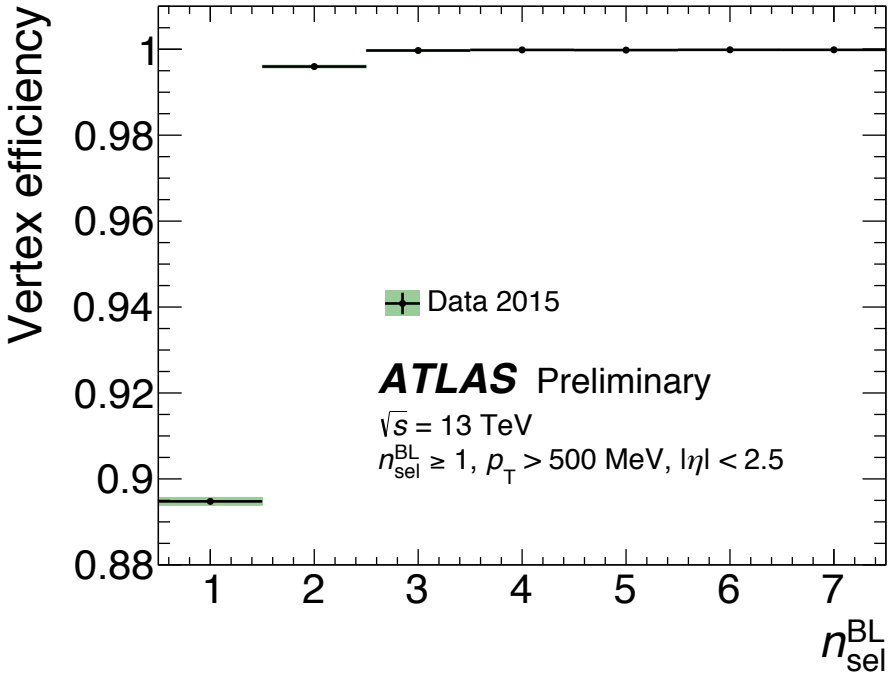

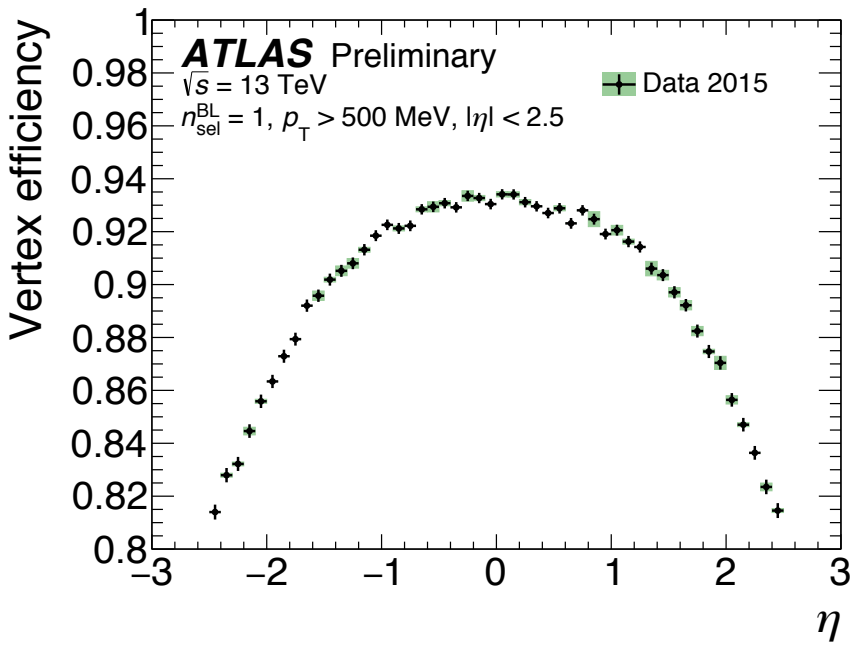

- The η dependence in n_{BL} = 1 varies from 81-93% for large |η| to small values
- Taken in account in the correction procedure

Non-Primary Tracks Estimation

- Non primary tracks are the biggest background
  - Rate measured in data by performing a fit to the transverse impact parameter distribution
  - 2.2% ± 0.6% of our reconstructed tracks within the signal region
- High pT tracks
  - measurable fraction of the tracks originate from low pT tracks (scattering, in flight decays)
  - the ability to select and remove these tracks was assessed in data
  - At most 1% of tracks between 30-50GeV

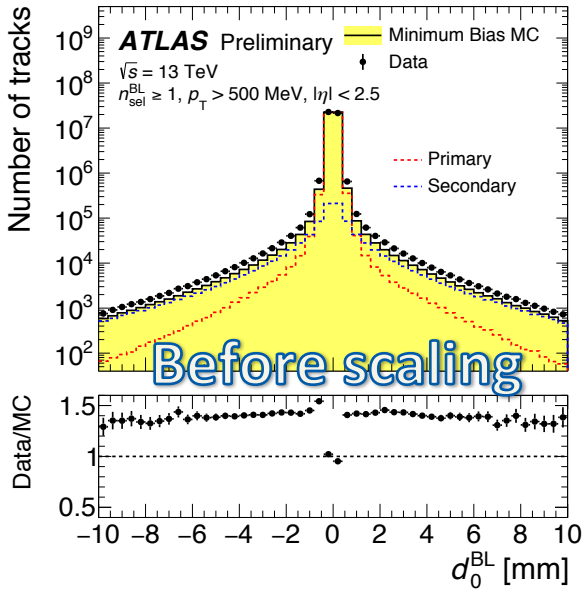

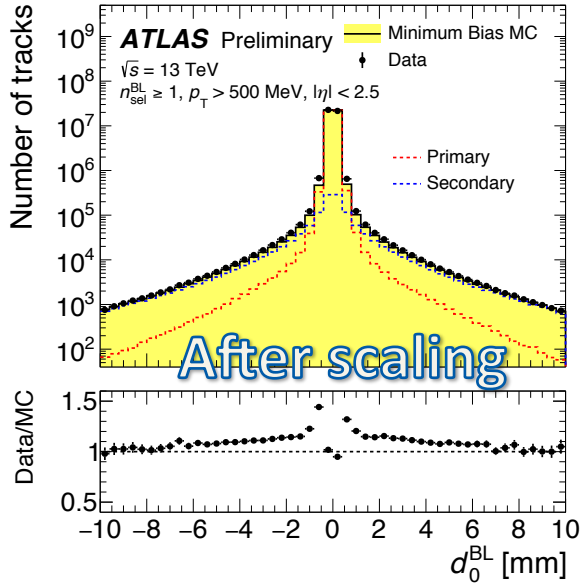

Final Results

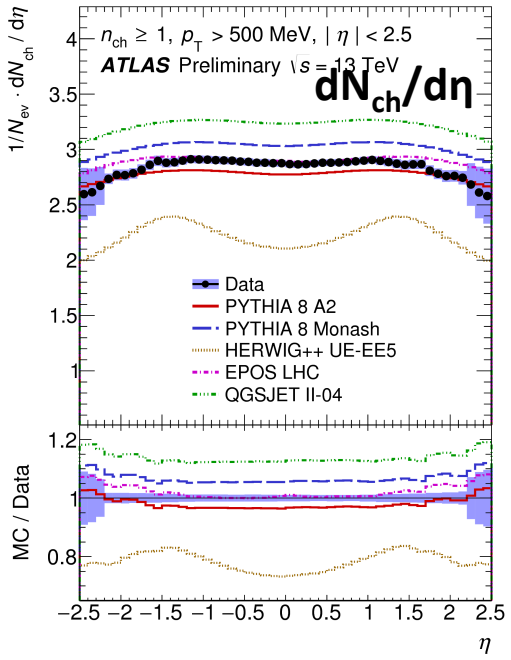

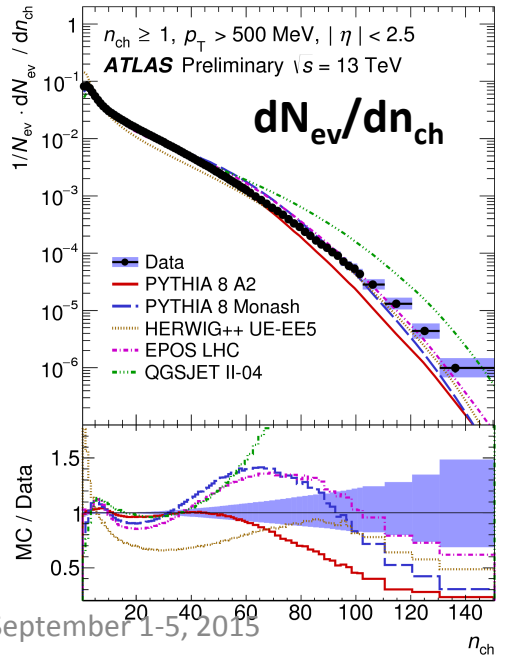

- Models differ mainly in normalisation, shape similar
  - Exception is HERWIG tuned entirely on UE
- Some Models/Tunes give remarkably good predictions (EPOS, Pythia)
- Low n_{ch} not well modelled by any MC; large contribution from diffraction
- Models without colour reconnection (QGSJET) fail to model scaling with n_{ch} very well

Generator	Version	Tune	PDF	7 TeV dat	
				MB	UE
PYTHIA 8	8.185	A2	MSTW2008LO [19]	yes	no
PYTHIA 8	8.186	MONASH	NNPDF2.3LO [20]	yes	yes
HERWIG++	2.7.1	UE-EE-5-CTEQ6L1	CTEQ6L1 [21]	no	yes
EPOS	3.1	LHC	N/A	yes	no
QGSJET-II	II-04	default	N/A	yes	no

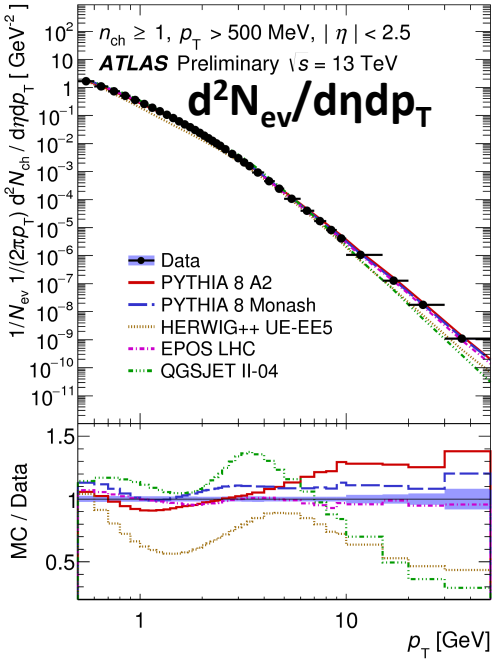

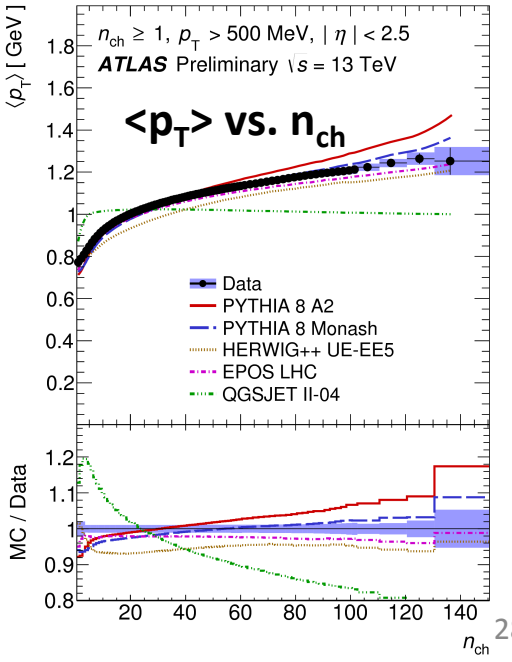

Tracking Systematic Uncertainties

$$\epsilon_{\mathrm{trk}}(p_{\mathrm{T}},\eta) = \frac{N_{\mathrm{rec}}^{\mathrm{matched}}(p_{\mathrm{T}},\eta)}{N_{\mathrm{gen}}(p_{\mathrm{T}},\eta)}$$

Systematic uncertainties (details in the next slides):

- N-1 cut efficiencies (MC versus data) for the number of hit requirements: **0.5%** systematic
- N-1 cut efficiency for χ2 prob. Cut: **0.5%** systematic for pT > 10 GeV
- Material description (dominant):
  a. Material constrained to ±5% from Run 1 → **1% (1.5%)** systematic in the **central (forward) region**
  b. Studies of conversions and secondary vertices from hadronic interactions indicate missing material in the IBL leading to **~1%** systematic
  c. SCT extension efficiency indicates possible missing material in the region |η| > 2.2 → **5%** systematic

b. and c. combined linearly and then add in quadrature with a.

N-1 cut Systematic Uncertainty

$$\epsilon_{\text{cut}}(p_{\text{T}},\eta) = \frac{N^{\text{tracks}}_{\text{all cuts}}(p_{\text{T}},\eta)}{N^{\text{tracks}}_{\text{N}-1\text{ cuts}}(p_{\text{T}},\eta)}$$

- All Pixel hit requirements and all SCT hit requirements removed for the N-1 test **0.5%**

- Large differences are observed at high p_T for the efficiency of both cuts, this is the result of a high fraction of poorly measured tracks entering the denominator when loosening the cuts

X^2 Probability Cut Systematic Uncertainty

- Badly measured low momentum charged particles are sometimes reconstructed as a high momentum track
- These tracks are a sizeable fraction at high reconstructed p_T because of the steeply falling p_T distribution and they are caused by interactions and multiple scattering with the material -> usually have a bad χ2 fit probability
- A cut on χ2 probability of $P(\chi 2, n_{dof}) > 0.01$ is applied for tracks with $p_T > 10$ GeV to remove bad measured tracks
- The uncertainty on the remaining amount of mis-measured tracks has been determined to be less than 0.2% at 10 GeV rising up to 7% above above 50 GeV
- The uncertainty in the efficiency of the cut is assessed to be to 0.5% below 50 GeV and 5% above 50 GeV

Material Systematic Uncertainty

- Hadrons have a high probability of hadronic interactions with the material of the inner detector -> the track reconstruction efficiency is heavily dependent on the material distribution in the detector

- Studies during Run-1 indicate that the material in the pixel detector and the SCT and TRT is known to a 5%-level or better

Now: new beam pipe, included the IBL, and the pixel patch panels updated -> it is necessary to re-estimate the material in the Inner Detector

Three data-driven methods are used to estimate the material systematic uncertainty:

- Hadronic Interactions Rate
- Photon Conversions Rate
- SCT Extension Efficiency

A detailed measurement of the material in the new beam pipe has been performed with X-rays and the material has been measured to a precision of 1%. Therefore no additional uncertainty is considered due to the new beam pipe.

Forward Material Uncertainty

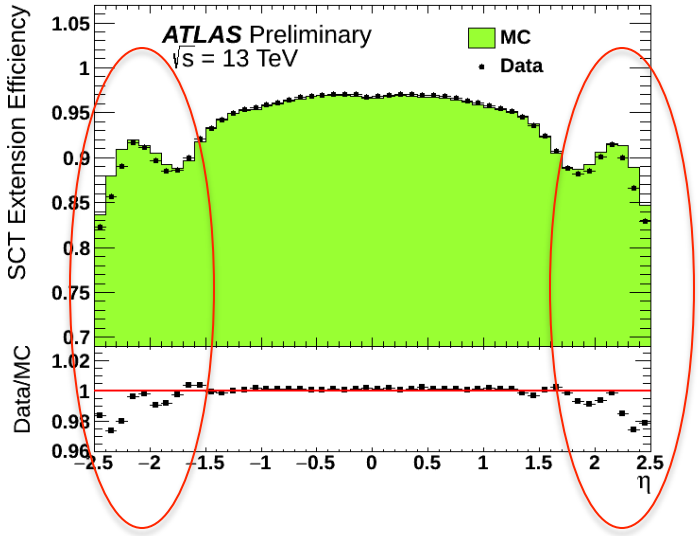

- Discrepancy > 2% in Data/MC comparison in the high eta regions (due to more than 10% of extra material missing in simulation)

- ~ 2% in the SCT Extension Efficiency ->
  ~ 5% in the Tracking Efficiency

Alignment Systematic Uncertainty

- MinBias is an early analysis: alignment of the ID is suboptimal due to limited data and time needed to refine the alignment
- Detector misalignments can be divided into two general categories:
  - χ2 invariant deformations
    can not be assessed with limited amounts of data and a conservative estimate based on the weak modes initially present in Run I has been used
  - deformations that impact the fit quality
    largely removed with early Run-2 data, and thus remaining misalignments can be quantified by comparing the track-hit residuals in data and MC simulation

Misalignments have no measurable effect on the track reconstruction efficiency or the acceptance of tracks in MinBias selection. The largest impact of ID misalignments is on the measured momentum of the reconstructed tracks:

- Random misalignments -> smearing of the momentum resolution
- systematic misalignments -> bias the reconstructed momentum

Both categories impact the measured momentum distribution of tracks. Four effects are considered to estimate the systematic uncertainty due to detector alignment

Negligible on Tracking Efficiency!

Conclusion: Combined Total Uncertainty

- The two uncertainties from the missing material in the IBL and in the forward region are added linearly and symmetrised then combined quadratically with the uncertainty from the constraint from Run 1

- This gives a total of 1.1% in the most central region and 6.5% in the most forward region

Systematics

The results from these and other studies are summarized in Table 6 which contains the systematic uncertainties applied to track reconstruction for all sources. All effects are assumed to be Gaussian and are added in quadrature.Figure 13 shows the total systematic uncertainty on track reconstruction efficiency as a function of track η and p_T. These systematic uncertainties are briefly discussed in the following subsections.

Systematic Uncertainty	Size	Region
Track Selection	0.5 %	flat in p_T and η
Material	2-8 %	decreases with p_T, increases with $\|\eta\|$
χ^2 prob. cut efficiency	0.5% - 5%	only for $p_T > 10$ GeV increases with p_T

Table 6: The systematic uncertainties on the track reconstruction efficiency. All uncertainties are quoted relative to the track reconstruction efficiency.

Table 7 summaries the impact of other track fit quality related issues on the final result. These effects do not impact the track reconstruction efficiency but do change the reliability of the simulation to emulate the data.

Systematic Uncertainty	Size	Region
χ^2 prob. cut remaining bad tracks	0.2% - 7%	only for $p_T > 10$ GeV increases with $\|\eta\|$ and p_T
Alignment and other high p_T	0.1-10%	only for $p_T > 10$ GeV averaged over η, increases with increasing p_T

Table 7: The systematic uncertainties on the final distributions due to track performance in data. All uncertainties are quoted relative to the total number of reconstructed or unfolded tracks.

Different Centre of Mass Energy

$dN_{ch}/d\eta$ http://arxiv.org/pdf/1012.5104v2.pdf

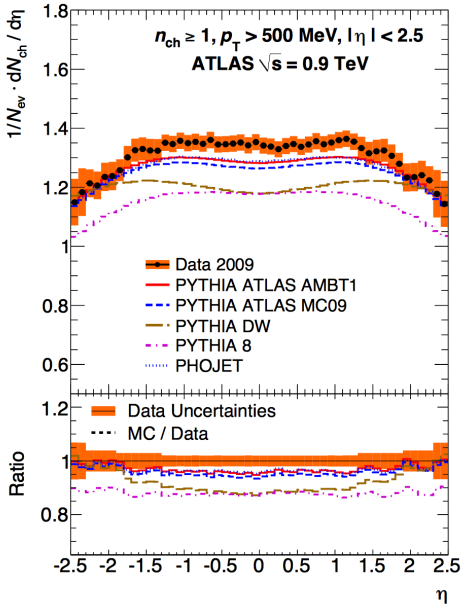

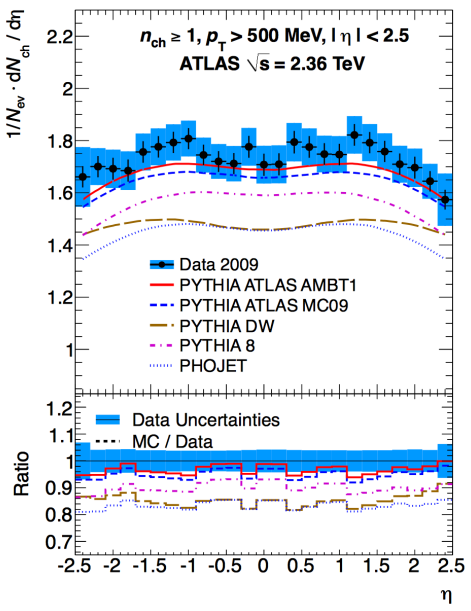

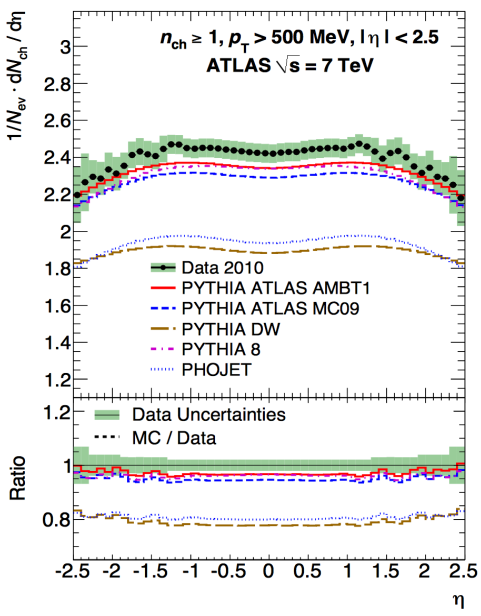

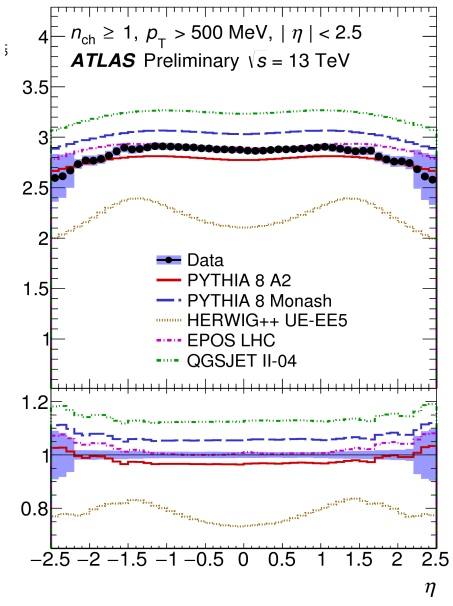

- Models differ mainly in normalisation, shape similar
- Track multiplicity underestimated

Different Centre of Mass Energy

$d^2N_{ev}/d\eta dp_T$ http://arxiv.org/pdf/1012.5104v2.pdf

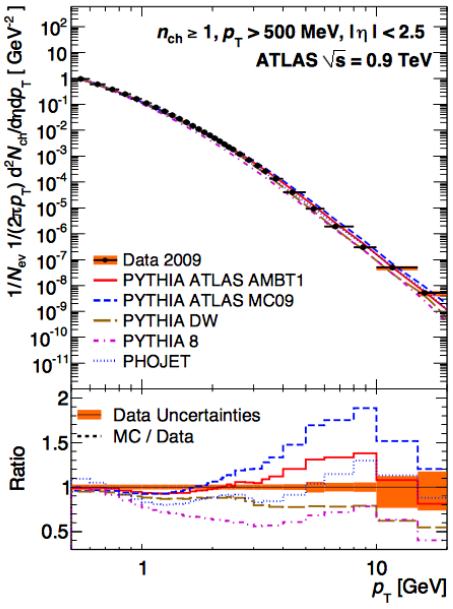

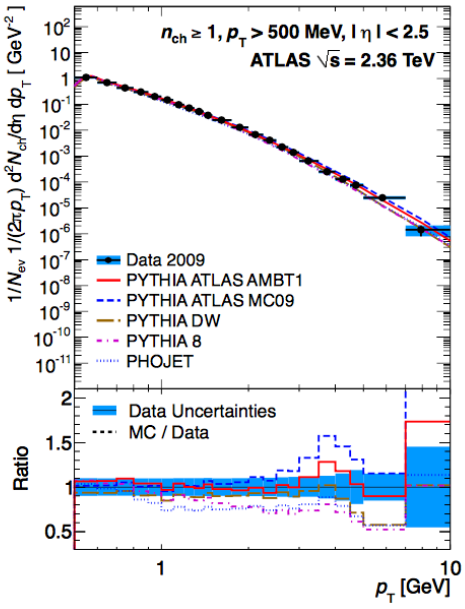

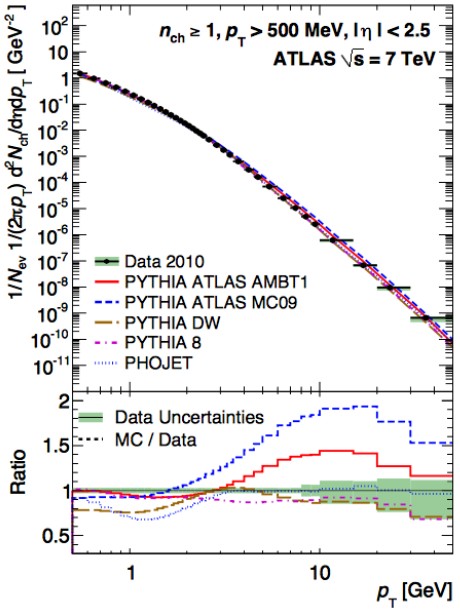

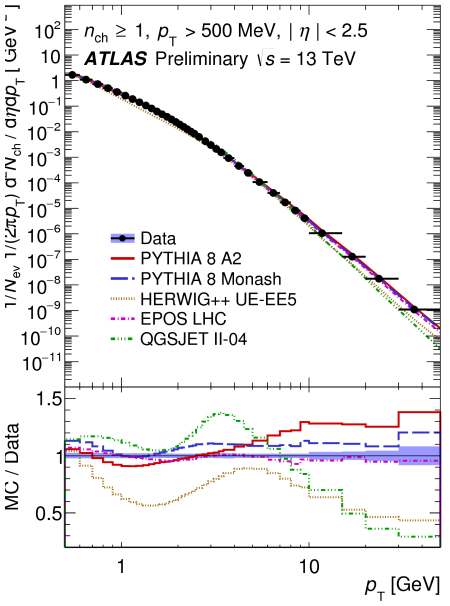

- Large disagreement at low p_T and high p_T

Different Centre of Mass Energy

dN_{ev}/dn_{ch} http://arxiv.org/pdf/1012.5104v2.pdf

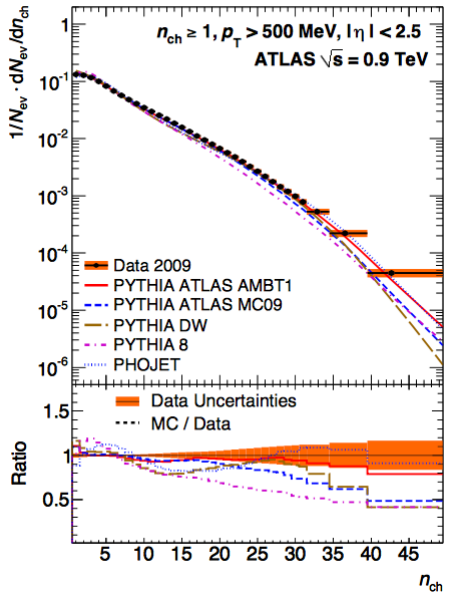

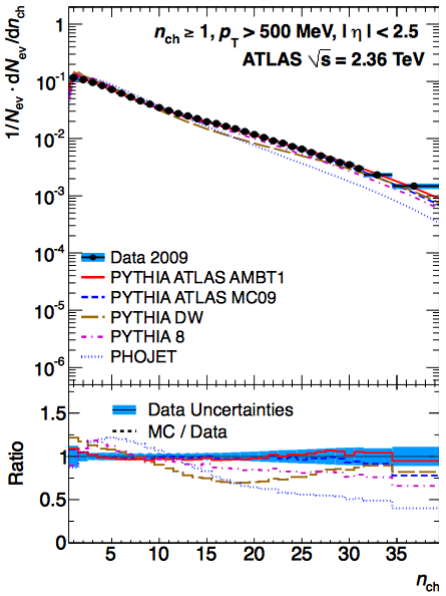

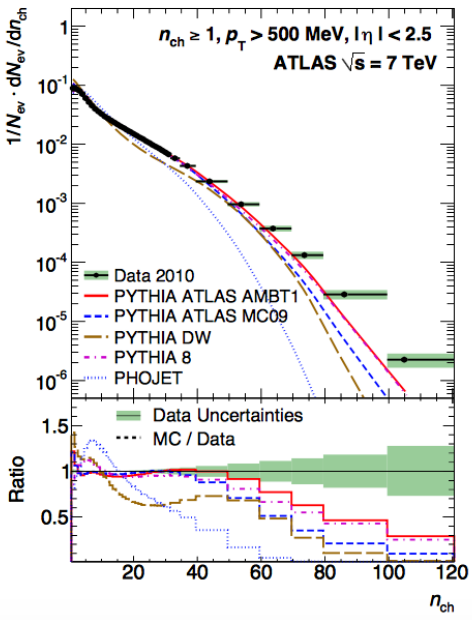

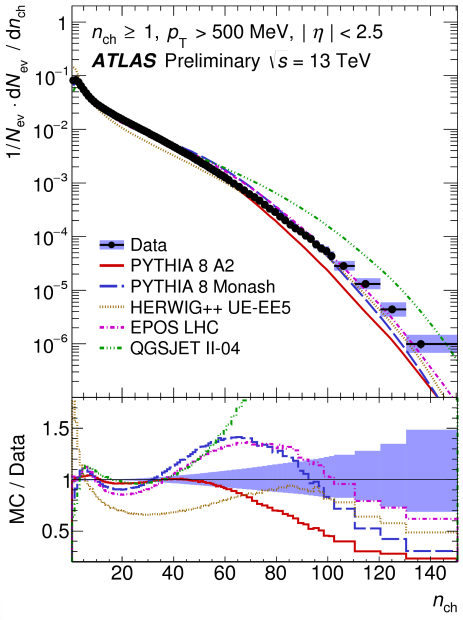

- Low n_{ch} not well modelled by any MC; large contribution from diffraction

Different Centre of Mass Energy

$\langle p_T \rangle$ vs. n_{ch} http://arxiv.org/pdf/1012.5104v2.pdf

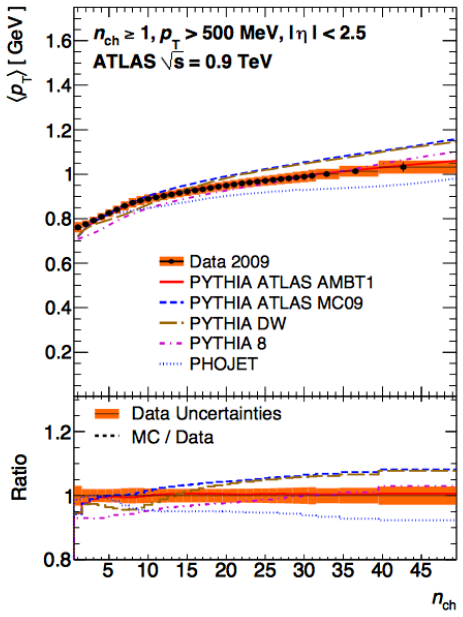

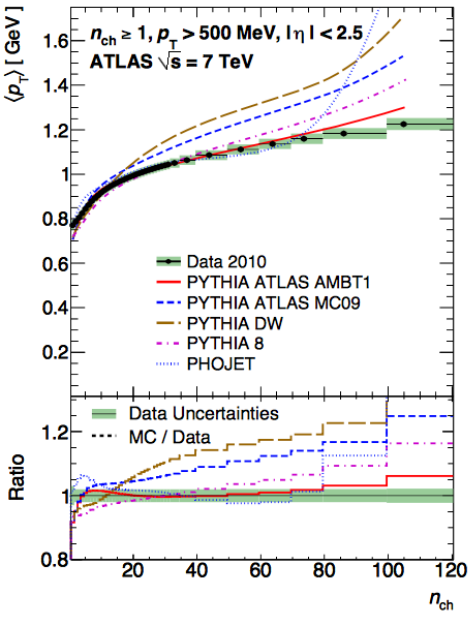

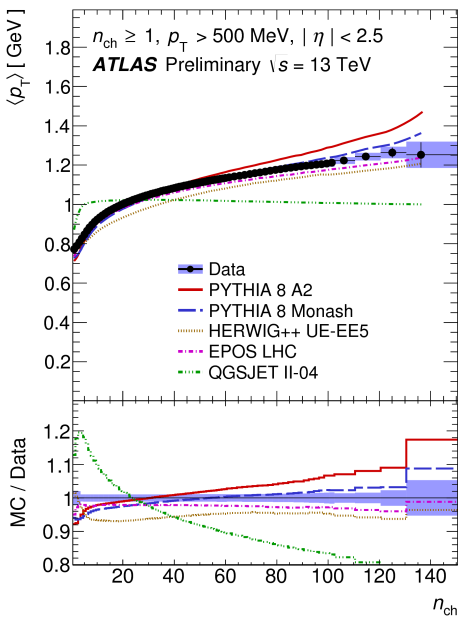

The measurement of ⟨pT⟩ as a function of charged multiplicity at s = 2.36 TeV is not shown because different track reconstruction methods are used for determining the p_T and multiplicity distributions

- Pythia8 with hard diffractive component give best description
- Shape at low n_{ch} sensitive to ND, SD, DD fractions especially when using a 100 MeV selection

Different Centre of Mass Energy

$\langle p_T \rangle$ vs. n_{ch} http://arxiv.org/pdf/1012.5104v2.pdf

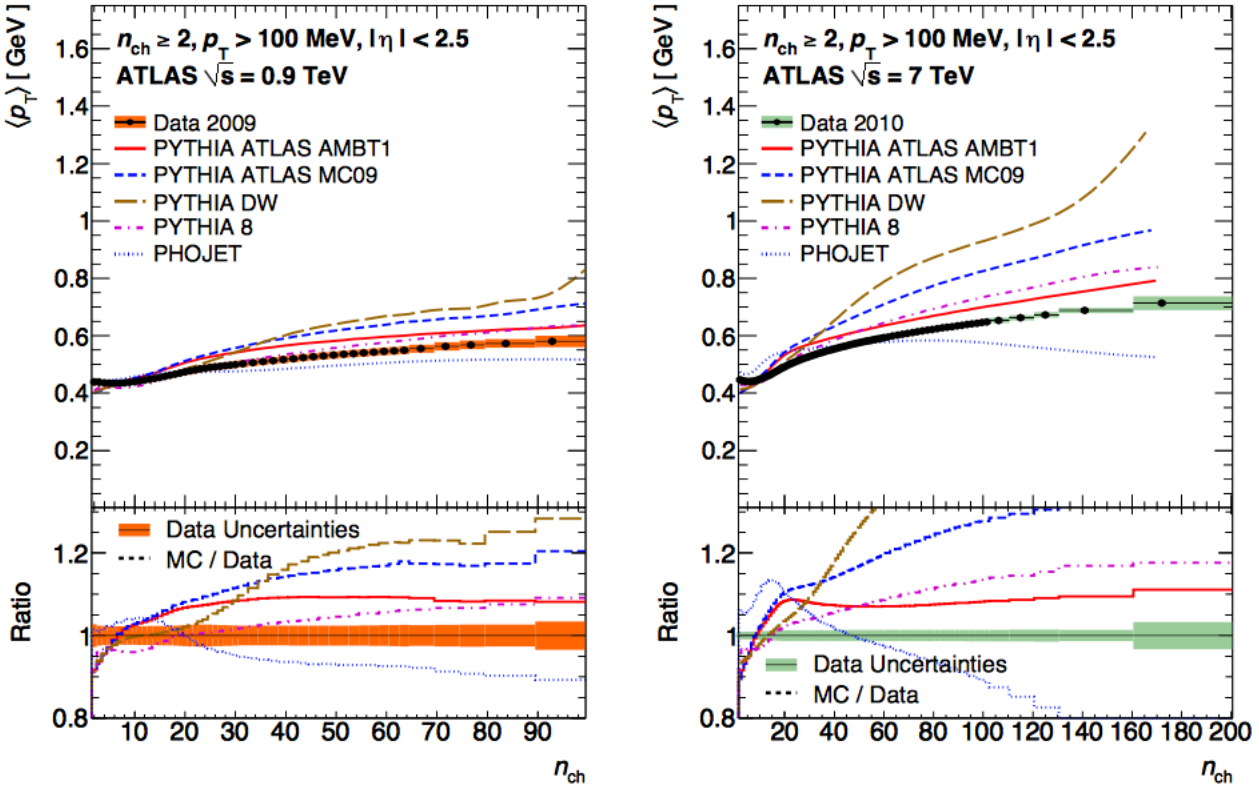

- Pythia8 with hard diffractive component give best description
- Shape at low n_{ch} sensitive to ND, SD, DD fractions especially when using a 100 MeV selection

Different Centre of Mass Energy

The measurement of ⟨pT⟩ as a function of charged multiplicity at s = 2.36 TeV is not shown because different track reconstruction methods are used for determining the p_T and multiplicity distributions

$\langle p_T \rangle$ vs. n_{ch} http://arxiv.org/pdf/1012.5104v2.pdf

4.3.2 Track Reconstruction Algorithms at 2.36 TeV

Operation of the SCT at standby voltage during 2.36 TeV data taking led to reduced SCT hit efficiency. Consequently, ID tracks are reconstructed at this centre-of-mass energy using looser requirements on the numbers of hits and holes [4] [44,45]. There are no simulation samples that fully describe the SCT operating at reduced voltage. A technique to emulate the impact of operating the SCT in standby was developed in simulation; this corrects the Monte Carlo without re-simulation by modifying the silicon clusterisation algorithm used to study the tracking performance. However, the final ID track efficiency at $\sqrt{s} = 2.36$ TeV was determined using a correction to the track reconstruction efficiency derived from data at $\sqrt{s} = 0.9$ TeV.

Pixel tracks were reconstructed using the standard track reconstruction algorithms limited to Pixel hits and with different track requirements. There is little redundant information, because at least three measurement points are needed to obtain a momentum measurement and the average number of Pixel hits per track is three in the barrel. Therefore the Pixel track reconstruction efficiency is very sensitive to the location of inactive Pixel modules. The total distance between the first and the last measurement point in the pixel detector, as well as the limited number of measurement points per track, limit the momentum resolution of the tracks; therefore the Pixel tracks were refit using the reconstructed primary vertex as an additional measurement point. The refitting improves the momentum resolution by almost a factor of two. However, the Pixel track momentum resolution remains a factor of three worse than the resolution of ID tracks.

The selection criteria used to define good Pixel and ID tracks are shown in Table 3. The total number of accepted events and tracks at this energy are shown in Table 4. These two track reconstruction methods have different limitations; the method with the best possible measurement for a given variable is chosen when producing the final plots. The Pixel track method is used for the n_{ch} and η distributions, while the ID track method is used for the p_T spectrum measurement; the $\langle p_T \rangle$ distribution is not produced for this energy as neither method is able to describe both the number of particles and their p_T accurately.

Underlying Events at 7 TeV: Jets -tunes-

http://arxiv.org/abs/1406.0392 **Leading Jet**

Table 2 Details of the MC models used in this paper. It should be noted that all tunes use data from different experiments for constraining different processes, but for brevity only the data which had most weight in each tune is listed. A "main data" value of "LHC" indicates data taken at $\sqrt{s} = 7$ TeV, although $\sqrt{s} = 900$ GeV data were also included with much smaller weight in the ATLAS tunes. Some tunes are focused on describing the minimum bias (MB) distributions better, while the rest are tuned to describe the underlying event (UE) distributions, as indicated in "focus". The detector-simulated MC configurations used for data correction are separated from those used in the results comparison plots, for clarity. For the POWHEG+PYTHIA 6 entry, separate parton distribution functions (PDFs) were used for the matrix element and parton shower / multiple scattering aspects of the modelling, indicated with "ME" and "PS/MPI" respectively.

Generator	Version	Tune	PDF	Focus	Main data	Used for
PYTHIA 8	8.157	AU2 [28]	CT10 [29]	UE	LHC	MC/data comparison
PYTHIA 6	6.425	Perugia 2011 [30]	CTEQ5L [31]	UE	LHC	MC/data comparison
PYTHIA 6	6.421	DW [32]	CTEQ5L	UE	Tevatron	MC/data comparison
HERWIG++	2.5.1	UE7-2 [33]	MRST LO** [34]	UE	LHC	MC/data comparison
HERWIG+JIMMY	6.510	AUET2 [35]	MRST LO**	UE	LHC	MC/data comparison
ALPGEN+HERWIG+JIMMY	2.13 + 6.510	AUET1 [35]	CTEQ6L1 [36]	UE	LHC	MC/data comparison
POWHEG+PYTHIA 6	r2169 + 6.425	Perugia 2011	CT10 (ME) + CTEQ5L (PS/MPI)	UE	LHC	MC/data comparison
PYTHIA 6	6.425	AMBT1 [37]	MRST LO* [38]	MB	Early LHC	Data correction
HERWIG++	2.5.0	LO*_JETS [39]	MRST LO*	UE	Tevatron	Correction systematics

Underlying Events at 7 TeV: Z-boson -tunes-

http://arxiv.org/abs/1409.3433

Table 2 Main features of the Monte-Carlo models used. The abbreviations ME, PS, MPI, LO and NLO respectively stand for matrix element, parton shower, multiple parton interactions, leading order and next to leading order in QCD.

Generator	Type	Version	PDF	Tune
PYTHIA 6	LO PS	6.425	CTEQ6L1 [29]	Perugia2011C [30]
PYTHIA 8	LO PS	8.165	CTEQ6L1	AU2 [31]
HERWIG++	LO PS	2.5.1	MRST LO** [32]	UE-EE-3 [33]
Sherpa	LO multi-leg ME + PS	1.4.0 /1.3.1	CT10 [34]	Default
ALPGEN + HERWIG +JIMMY	LO multi-leg ME + PS (adds MPI)	2.14 6.520 4.31	CTEQ6L1 MRST LO**	AUET2 [35]
POWHEG + PYTHIA 8	NLO ME + PS	- 8.165	CT10 CT10	AU2

Underlying Events at 7 TeV: Jets -systematics-

http://arxiv.org/abs/1406.0392 **Leading Jet**

Table 3 Summary of systematic uncertainties for inclusive jet and exclusive dijet profiles vs. $p_{\mathrm{T}}^{\mathrm{lead}}$. The "efficiency" uncertainties include material uncertainties in the tracker and calorimeter geometry modelling. The "JES" uncertainty source for jets refers to the jet energy scale calibration procedure [50].

Quantity	Inclusive jets			Exclusive dijets		
	Pile-up and merged vertices			Pile-up and merged vertices		
All observables	1–3%			1–5%		
Charged tracks	Unfolding	Efficiency		Unfolding	Efficiency	
$\sum p_{\mathrm{T}}$	3%	1–7%		3–13%	2–7%	
N_{ch}	1–2%	3–4%		3–22%	3–7%	
mean p_{T}	1%	0–4%		1–9%	1%	
Calo clusters	Unfolding	Efficiency		Unfolding	Efficiency	
$\sum E_{\mathrm{T}}$, $\lvert\eta\rvert < 4.8$	2–3%	4–6%		5–21%	4–9%	
$\sum E_{\mathrm{T}}$, $\lvert\eta\rvert < 2.5$	3–5%	4–6%		1–21%	4–7%	
Jets	Energy resolution	JES	Efficiency	Energy resolution	JES	Efficiency
$p_{\mathrm{T}}^{\mathrm{lead}}$	0.3–1%	0.3–4%	0.1–2%	0.4–3%	1–3%	0.3–3%

Underlying Events at 7 TeV: Z-boson -systematics-

http://arxiv.org/abs/1409.3433

Table 3 Typical contributions to the systematic uncertainties (in %) on the unfolded and corrected distributions of interest in the toward and transverse regions for the profile distributions. The range of values in the columns 3 – 5 indicate the variations as a function of $p_{\mathrm{T}}^{\mathrm{Z}}$, while those in the last column indicate the variations as a function of N_{ch}. The column labelled *Correlation* indicates whether the errors are treated as correlated or not between the electron and muon channels.

Observable	Correlation	N_{ch} vs $p_{\mathrm{T}}^{\mathrm{Z}}$	$\sum p_{\mathrm{T}}$ vs $p_{\mathrm{T}}^{\mathrm{Z}}$	Mean p_{T} vs $p_{\mathrm{T}}^{\mathrm{Z}}$	Mean p_{T} vs N_{ch}
Lepton selection	No	0.5 – 1.0	0.1 – 1.0	< 0.5	0.1 – 2.5
Track reconstruction	Yes	1.0 – 2.0	0.5 – 2.0	< 0.5	< 0.5
Impact parameter requirement	Yes	0.5 – 1.0	1.0 – 2.0	0.1 – 2.0	< 0.5
Pile-up removal	Yes	0.5 – 2.0	0.5 – 2.0	< 0.2	0.2 – 0.5
Background correction	No	0.5 – 2.0	0.5 – 2.0	< 0.5	< 0.5
Unfolding	No	0.5 – 3.0	0.5 – 3.0	< 0.5	0.2 – 2.0
Electron isolation	No	0.1 – 1.0	0.5 – 2.0	0.1 – 1.5	< 1.0
Combined systematic uncertainty		1.0 – 3.0	1.0 – 4.0	< 1.0	1.0 – 3.5

Underlying Events at 13 TeV: -tunes-

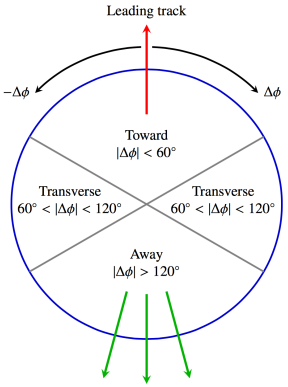

Table 2: Details of the MC models used. It is emphasized that the tunes use data from different experiments to constrain different processes, but for brevity only the *data* which had the most weight in each specific tune are shown. Some tunes are focused on describing the minimum-bias (MB) distributions better, while the rest are tuned to describe the underlying event (UE) distributions, as indicated. Except for A2 and A14, the tunes were performed by the MC developers

Generator	Version	Tune	PDF	Focus
Pythia8 [18]	8.186	A2 [19]	MSTW2008LO [20]	MB
Pythia8	8.186	Monash [21]	NNPDF2.3LO [22]	MB/UE
Pythia8	8.186	A14 [23]	NNPDF2.3LO	UE/Shower
Herwig++ [24]	2.7.1	UEEE5 [25]	CTEQ6L1 [26]	UE
Epos [27]	3.1	LHC [28]		MB

Underlying Events at 13 TeV
Σp_T and N_{ch} VS p_T

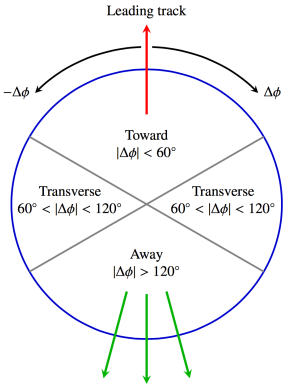

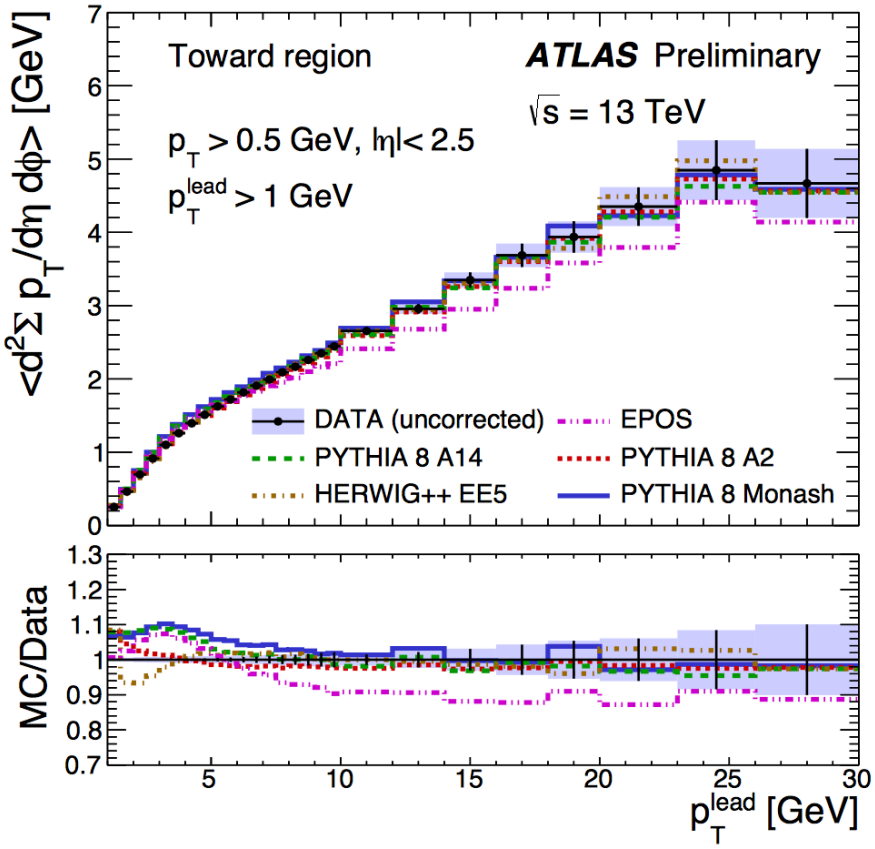

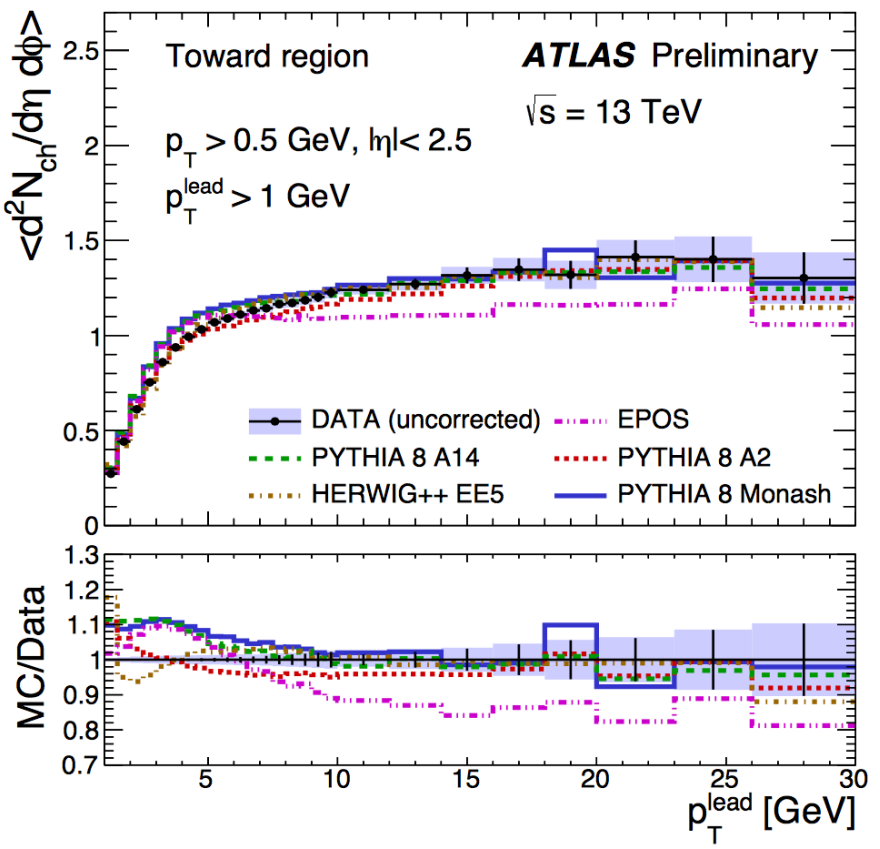

arXiv:1502.07947

Bose-Einstein Correlation

- Systematics on lambda and R for the exponential fit of the two particle double-ratio correlation function $R_2(Q)$

	0.9 TeV		7 TeV		7 TeV (HM)	
Source	λ	R	λ	R	λ	R
Track reconstruction efficiency	0.6%	0.7%	0.3%	0.2%	1.3%	0.3%
Track splitting and merging	negligible		negligible		negligible	
Monte Carlo samples	14.5%	12.9%	7.6%	10.4%	5.1%	8.4%
Coulomb correction	2.6%	0.1%	5.5%	0.1%	3.7%	0.5%
Fitted range of Q	1.0%	1.6%	1.6%	2.2%	5.5%	6.0%
Starting value of Q	0.4%	0.3%	0.9%	0.6%	0.5%	0.3%
Bin size	0.2%	0.2%	0.9%	0.5%	4.1%	3.4%
Exclusion interval	0.2%	0.2%	1%	0.6%	0.7%	1.1%
Total	14.8%	13.0%	9.6%	10.7%	9.4%	10.9%

arXiv:1502.07947

Bose-Einstein Correlation

- Results

BEC param.	Fit function	0.9 TeV	7 TeV Minimum-bias events	7 TeV High-multiplicity events
$R(n_{ch})$	$p_0 \sqrt[3]{n_{ch}}$	$p_0 = 0.64 \pm 0.07$ fm $(n_{ch} \leq 82)$	$p_0 = 0.63 \pm 0.05$ fm $(n_{ch} < 55)$	—
	p_0	—		$p_0 = 2.28 \pm 0.32$ fm $(n_{ch} \geq 55)$
$\lambda(n_{ch})$	$p_0 e^{-p_1 n_{ch}}$	$p_0 = 1.06 \pm 0.10$ $p_1 = 0.011 \pm 0.004$	$p_0 = 0.96 \pm 0.07$ $p_1 = 0.0038 \pm 0.0008$	
$R(k_T)$	$p_0 e^{-p_1 k_T}$	$p_0 = 2.64 \pm 0.33$ fm $p_1 = 1.48 \pm 0.67$ GeV^{-1}	$p_0 = 2.88 \pm 0.27$ fm $p_1 = 1.05 \pm 0.58$ GeV^{-1}	$p_0 = 3.39 \pm 0.54$ fm $p_1 = 0.92 \pm 0.73$ GeV^{-1}
$\lambda(k_T)$	$p_0 e^{-p_1 k_T}$	$p_0 = 1.20 \pm 0.18$ $p_1 = 2.00 \pm 0.35$ GeV^{-1}	$p_0 = 1.12 \pm 0.10$ $p_1 = 1.54 \pm 0.26$ GeV^{-1}	$p_0 = 0.75 \pm 0.10$ $p_1 = 0.91 \pm 0.45$ GeV^{-1}

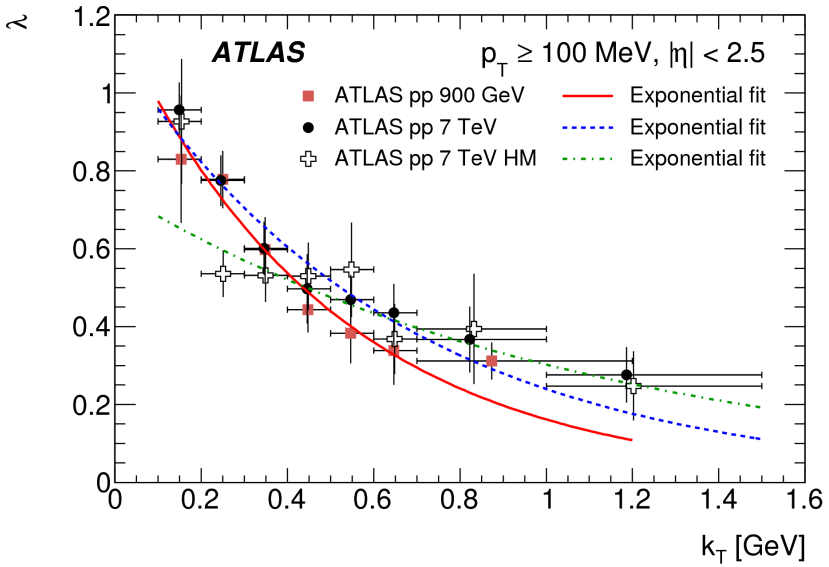

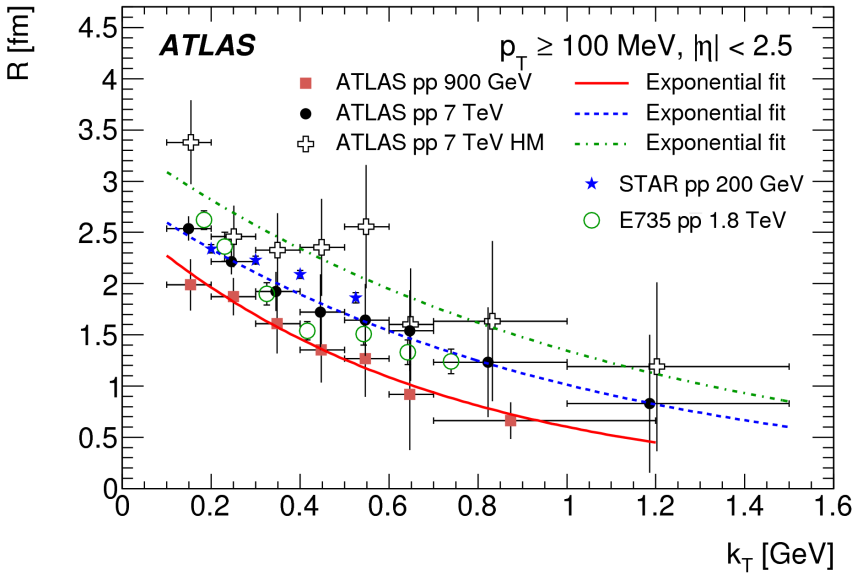

arXiv:1502.07947

Bose-Einstein Correlation

- Results

BEC param.	Fit function	0.9 TeV	7 TeV	
			Minimum-bias events	High-multiplicity events
$R(n_{ch})$	$p_0 \sqrt[3]{n_{ch}}$	$p_0 = 0.64 \pm 0.07$ fm $(n_{ch} \leq 82)$	$p_0 = 0.63 \pm 0.05$ fm $(n_{ch} < 55)$	—
	p_0	—	$p_0 = 2.28 \pm 0.32$ fm $(n_{ch} \geq 55)$	
$\lambda(n_{ch})$	$p_0\, e^{-p_1 n_{ch}}$	$p_0 = 1.06 \pm 0.10$ $p_1 = 0.011 \pm 0.004$	$p_0 = 0.96 \pm 0.07$ $p_1 = 0.0038 \pm 0.0008$	
$R(k_T)$	$p_0\, e^{-p_1 k_T}$	$p_0 = 2.64 \pm 0.33$ fm $p_1 = 1.48 \pm 0.67$ GeV^{-1}	$p_0 = 2.88 \pm 0.27$ fm $p_1 = 1.05 \pm 0.58$ GeV^{-1}	$p_0 = 3.39 \pm 0.54$ fm $p_1 = 0.92 \pm 0.73$ GeV^{-1}
$\lambda(k_T)$	$p_0\, e^{-p_1 k_T}$	$p_0 = 1.20 \pm 0.18$ $p_1 = 2.00 \pm 0.35$ GeV^{-1}	$p_0 = 1.12 \pm 0.10$ $p_1 = 1.54 \pm 0.26$ GeV^{-1}	$p_0 = 0.75 \pm 0.10$ $p_1 = 0.91 \pm 0.45$ GeV^{-1}

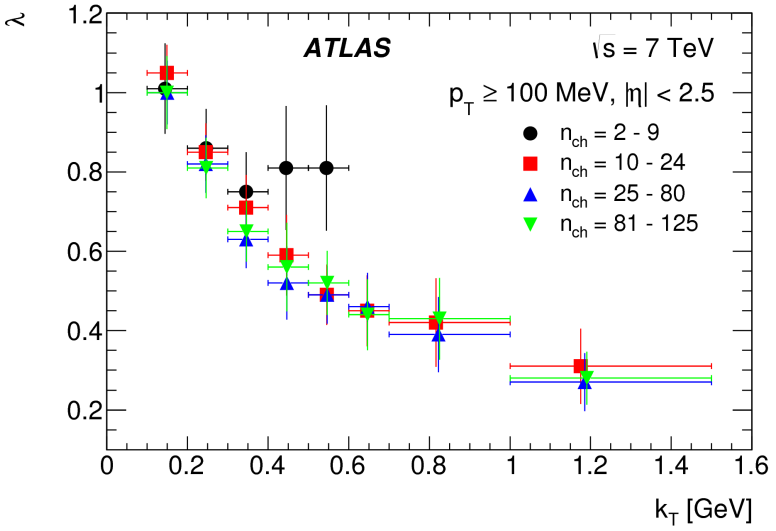

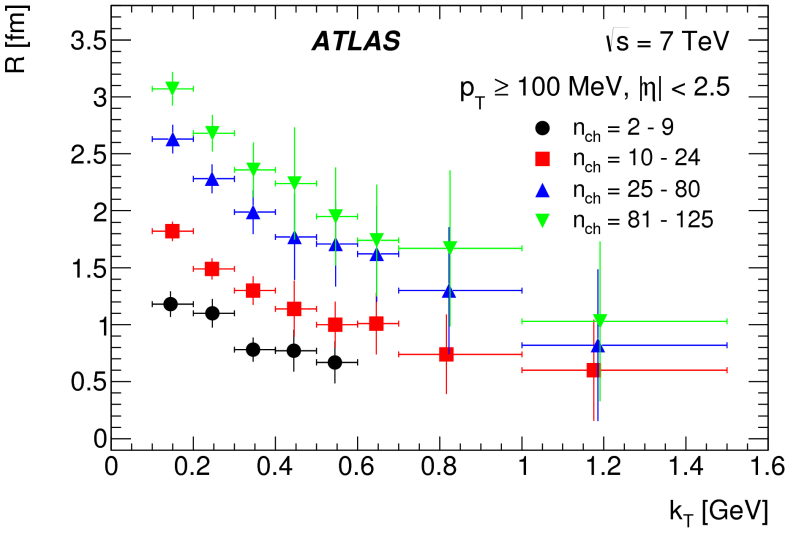

arXiv:1502.07947

Λ polarisation in the transverse plane

TABLE III. Transverse polarization of Λ and $\bar{\Lambda}$ measured in the full fiducial phase space and in bins of x_F and p_T. The values of $\bar{x}_F$ and $\bar{p}_T$ are mean values of x_F and p_T, respectively, in given ranges. The table lists both the statistical and systematic uncertainties.

Sample	$\bar{x}_F$	$\bar{p}_T$	Polarization	
	$[10^{-4}]$	[GeV]	Λ	$\bar{\Lambda}$
Full fiducial volume	10.0	1.91	$-0.010 \pm 0.005 \pm 0.004$	$0.002 \pm 0.006 \pm 0.004$
$x_F \in (0.5, 5) \times 10^{-4}$	2.8	1.83	$0.005 \pm 0.009 \pm 0.006$	$-0.009 \pm 0.010 \pm 0.006$
$x_F \in (5, 10.5) \times 10^{-4}$	7.5	1.85	$-0.012 \pm 0.009 \pm 0.008$	$0.002 \pm 0.010 \pm 0.007$
$x_F \in (10.5, 100) \times 10^{-4}$	19.3	2.12	$-0.005 \pm 0.010 \pm 0.008$	$0.012 \pm 0.010 \pm 0.010$
$p_T \in (0.8, 1.3)$ GeV	7.5	1.07	$-0.008 \pm 0.012 \pm 0.011$	$-0.004 \pm 0.013 \pm 0.013$
$p_T \in (1.3, 2.03)$ GeV	9.3	1.64	$-0.019 \pm 0.009 \pm 0.007$	$-0.003 \pm 0.010 \pm 0.007$
$p_T \in (2.03, 15)$ GeV	12.6	2.84	$-0.005 \pm 0.008 \pm 0.005$	$0.009 \pm 0.009 \pm 0.004$

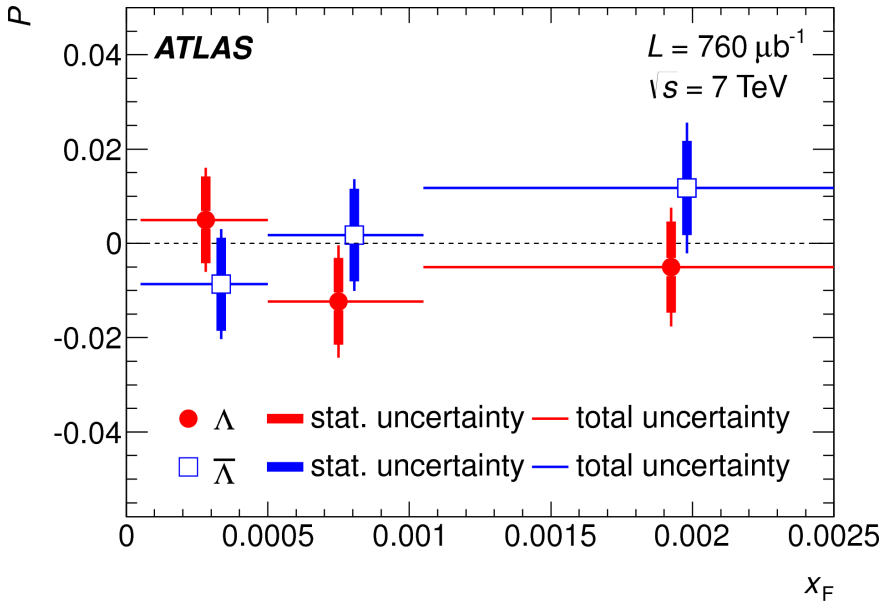

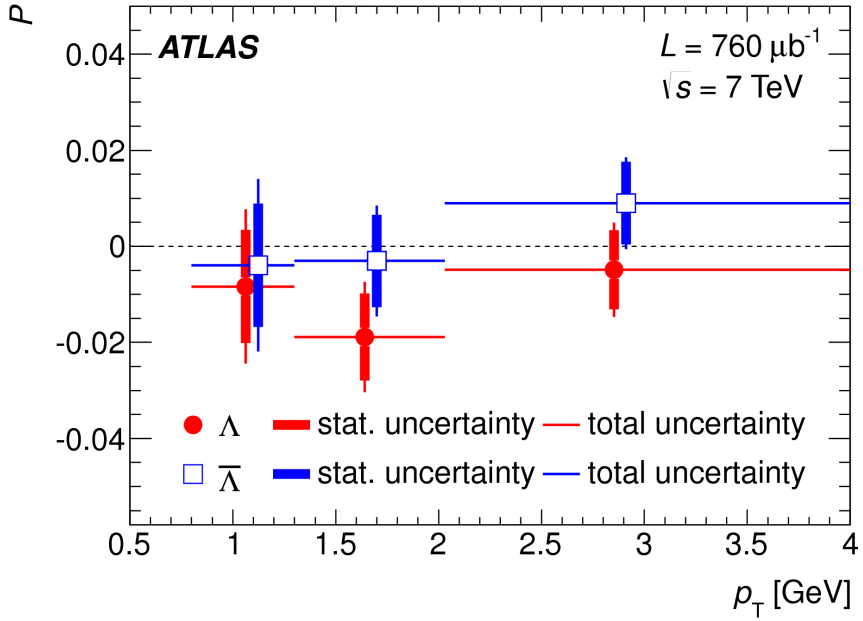

arXiv:1502.07947

Λ polarisation in the transverse plane

TABLE II. Summary of systematic uncertainties. The numbers represent absolute systematic uncertainties of the polarization values. All negligible systematic uncertainties are summarized under "Other contributions". Individual values before rounding are added in quadrature to obtain the total systematic uncertainty.

Systematic uncertainty	Λ	$\bar{\Lambda}$
MC statistics	0.003	0.003
Mass range	0.003	0.003
Background	0.001	0.001
Kinematic weighting	0.001	0.001
Other contributions	$< 5 \times 10^{-4}$	$< 5 \times 10^{-4}$
Total	0.004	0.004

arXiv:1502.07947

Λ polarisation in the transverse plane: comparison with other experiments

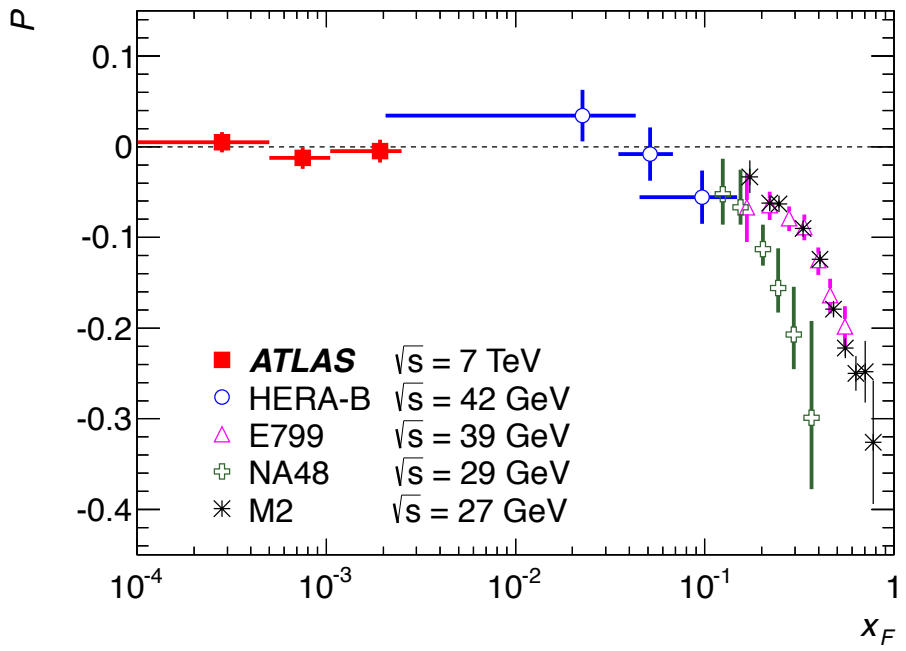

Figure 8 compares this result with other measurements: an experiment at the M2 beam-line at Fermilab [2], experiment E799 [3] also at Fermilab, NA48 [4] at CERN, and HERA-B [5] at DESY. Direct comparison of results from different experiments is non-trivial, since each measurement was made at a different center-of-mass energy and covers a different phase space: the average p_{T} coverage of the M2 experiment is 0.62–1.74 GeV, the p_{T} range of the E799 experiment is 0.67–2.15 GeV, NA48 covers p_{T} of 0.28–0.86 GeV, HERA-B 0.82–0.84 GeV, and in Fig. 8 the ATLAS data cover the average p_{T} range of 1.83–2.12 GeV. Furthermore, the HERA-B measurement covers negative values of x_{F}. In Fig. 8, the HERA-B results are transformed using Eq. (1) so that they can be compared with other results. The E799 and NA48 experiments define x_{F} as the fraction of the beam energy carried by the Λ. In Fig. 8, the values are transformed according to the definition of x_{F} used in this paper (although the difference is very small). Figure 8 shows only a subset of the M2 results measured at a fixed production angle of about 6 mrad with a beryllium target. A parameterization of the polarization [2] as a function of x_{F} and p_{T} is used to extrapolate the results of the M2 experiment to the x_{F} and p_{T} range of this measurement. The extrapolated value is less than 5×10^{-4}, which can effectively be treated as zero given the precision of this measurement.